Monthly Notices
of the
ROYAL ASTRONOMICAL SOCIETY

MNRAS **436,** 774–795 (2013)
Advance Access publication 2013 October 1

doi:10.1093/mnras/stt1612

The death of massive stars – II. Observational constraints on the progenitors of Type Ibc supernovae

John J. Eldridge,[1]⋆ Morgan Fraser,[2] Stephen J. Smartt,[2] Justyn R. Maund[2] and R. Mark Crockett[2]

[1]*The Department of Physics, The University of Auckland, Private Bag 92019, Auckland, New Zealand*
[2]*Astrophysics Research Centre, School of Mathematics and Physics, Queen's University Belfast, Belfast BT7 1NN, UK*

Accepted 2013 August 23. Received 2013 August 23; in original form 2013 January 4

ABSTRACT

The progenitors of many Type II core-collapse supernovae (SNe) have now been identified directly on pre-discovery imaging. Here, we present an extensive search for the progenitors of Type Ibc SNe in all available pre-discovery imaging since 1998. There are 12 Type Ibc SNe with no detections of progenitors in either deep ground-based or *Hubble Space Telescope* archival imaging. The deepest absolute *BVR* magnitude limits are between −4 and −5 mag. We compare these limits with the observed Wolf–Rayet population in the Large Magellanic Cloud and estimate a 16 per cent probability that we have failed to detect such a progenitor by chance. Alternatively, the progenitors evolve significantly before core-collapse or we have underestimated the extinction towards the progenitors. Reviewing the relative rates and ejecta mass estimates from light-curve modelling of Ibc SNe, we find both incompatible with Wolf–Rayet stars with initial masses $>25\,M_{\odot}$ being the only progenitors. We present binary evolution models that fit these observational constraints. Stars in binaries with initial masses $\lesssim 20\,M_{\odot}$ lose their hydrogen envelopes in binary interactions to become low-mass helium stars. They retain a low-mass hydrogen envelope until $\approx 10^4$ yr before core-collapse; hence, it is not surprising that Galactic analogues have been difficult to identify.

Key words: binaries: general – stars: evolution – supergiants – supernovae: general – stars: Wolf–Rayet.

1 INTRODUCTION

Massive stars live fast and die young; core-collapse supernovae (CCSNe) are the dramatic explosions which mark their deaths. During these events, a large amount of energy is deposited into the surrounding interstellar medium (ISM), while elements heavier than boron are created through explosive nucleosynthesis. The physical mechanism of core-collapse in a star with an iron core is well established as the main driving source behind the vast majority of core-collapse explosions (Janka 2012; Burrows 2013). However, the structure of the star before explosion and the variety in explosions (kinetic energies, luminosities and variation in the production of radioactive ^{56}Ni) are still not well understood. The observational characteristics are critically affected by the evolutionary history of its progenitor star and uncertainties remain (most notably in convection, mass-loss and rotation) that limit our quantitative understanding (see Langer 2012 for a discussion of current limitations).

Observed supernovae (SNe) are first divided into Types I and II, based, respectively, on the absence or presence of hydrogen in the early-time optical spectrum (Filippenko 1997; Turatto, Benetti & Pastorello 2007). These two broad types are further divided into several subtypes. The most common Type II SNe are Type IIP, characterized by a long plateau phase in their light curve of constant luminosity, which lasts for several months. The light curves of Type IIL SNe exhibit a linear decay, while Type IIb SNe only show hydrogen in their spectra for the first few weeks before it disappears. Type IIn SNe are slightly different; the hydrogen is seen as narrow (<100 km s^{-1}) emission lines, which arise from interaction with dense, optically thick circumstellar material. Type Ia SNe are hydrogen- and helium-poor SNe that are believed to be thermonuclear explosions arising as a result of accretion on to a carbon–oxygen white dwarf and are not considered further here (see Hillebrandt & Niemeyer 2000 for a review). The other hydrogen-poor Type I SNe are subdivided into Types Ib and Ic, which either do or do not show helium in their spectra, respectively. The Type Ibc SNe[1] have long been associated with Wolf–Rayet (WR) progenitors (e.g. Begelman & Sarazin 1986; Gaskell et al. 1986).

⋆E-mail: j.eldridge@auckland.ac.nz

[1] The Types Ib and Ic are often difficult to distinguish and their classification is dependent on the phase of the spectra and signal-to-noise. Hence, we will often use the common term of Type Ibc to cover them jointly.

In Paper I of this series, Smartt et al. (2009), the progenitors of Type IIP SNe were identified as red supergiants (RSGs) with massive and extended hydrogen envelopes. This conclusion was based on an analysis of pre-explosion images [mostly from the *Hubble Space Telescope* (*HST*)] for 20 nearby SNe. These images were used to detect or place limits on the luminosity and thus the mass of the progenitors. For the other subclasses of Type II SNe, there are some detections, but insufficient numbers to consider in detail as an ensemble. There have been three detected Type IIb progenitors for SNe 1993J, 2008ax and 2011dh, one transitional Type IIP/L progenitor for SN 2009kr and a progenitor detected for the peculiar Type II SN 1987A (Walborn et al. 1987; Aldering, Humphreys & Richmond 1994; Maund et al. 2004, 2011; Crockett et al. 2007; Elias-Rosa et al. 2010; Fraser et al. 2010; Arcavi et al. 2011). Together, these observations suggest that if the progenitors of Type II SNe are not RSGs, they are of a similar luminosity but with a different surface temperature ranging from blue supergiants (BSGs) to yellow supergiants (YSGs).

Besides Type IIP SNe, the only other SNe for which there are a large number of pre-explosion images available are the hydrogen-deficient Type Ibc SNe. There have been many attempts to directly identify the progenitors of Ibc SNe in these pre-discovery images, but no success (see Van Dyk, Li & Filippenko 2003a; Gal-Yam et al. 2005; Maund & Smartt 2005; Maund, Smartt & Schweizer 2005; Crockett et al. 2007, 2008). A luminous outburst or eruption from a progenitor star for the Type Ibn SN2006jc was detected (Foley et al. 2007; Pastorello et al. 2007), but the progenitor was not detected in a quiescent phase. The progenitors of Type Ibc SNe could potentially be the classical, massive WR stars which are initially massive ($M_{\rm ZAMS} \gtrsim 25$–$30\,{\rm M}_{\odot}$) but then lose their hydrogen envelopes through radiatively driven stellar winds (Crowther 2007). Such mass-loss in massive stars can also be enhanced in massive binary systems.

Alternatively, it has been suggested that progenitors of Type Ibc SNe could be helium stars with zero-age main-sequence (ZAMS) masses that are too low to allow a *single* star to enter the WR stage. In these cases, the star could have an initial mass of significantly less than $\lesssim 25\,{\rm M}_{\odot}$. The lower initial mass limit for an SN progenitor in such a system is uncertain, but is probably around the limit for single stars to produce Fe cores, or O–Mg–Ne cores, around $8\,{\rm M}_{\odot}$ (Smartt 2009). Such a star could lose its hydrogen envelope through interaction with a binary companion, losing mass by Roche lobe overflow or common-envelope evolution (e.g. Paczyński 1967; Iben & Tutukov 1985; Podsiadlowski, Joss & Hsu 1992; Tutukov, Yungelson & Iben 1992; Nomoto, Iwamoto & Suzuki 1995; De Donder & Vanbeveren 1998; Belczynski, Kalogera & Bulik 2002; Vanbeveren, Van Bever & Belkus 2007). While theoretically such stars are likely progenitors of Type Ibc SNe, there are no direct hydrogen-free analogues in our own galaxy, which has led to some scepticism as to their existence. The closest such systems we are aware of are V Sagittae systems, WR7a and HD 45166, which retain some hydrogen on their surfaces (e.g. Steiner & Diaz 1998; Oliveira, Steiner & Cieslinski 2003; Steiner & Oliveira 2005; Groh, Oliveira & Steiner 2008). However, a recently refined measurement of the relative rates of the SN types, together with modelling of the evolution of binary systems, has added weight to the argument that these binary stars represent a significant fraction of Type Ibc progenitors (e.g. De Donder & Vanbeveren 1998; Eldridge, Izzard & Tout 2008; Yoon, Woosley & Langer 2010; Eldridge, Langer & Tout 2011; Smith et al. 2011a).

In this paper, we combine the observed upper limits on the luminosity of individual Type Ibc progenitors with theoretical modelling of a binary population to constrain the progenitor population as a whole. In particular, we aim to determine whether the observed magnitude limits for Type Ibc SN progenitors (and their relative rates) can be reconciled with the observed population of WR stars in the Milky Way and Magellanic Clouds, or whether they are better matched by a model population including binary and single stars.

2 THE LOCAL SN RATE

We have followed the methodology of Paper I in sample selection. The list of SNe maintained by the International Astronomical Union (IAU) Central Bureau for Astronomical Telegrams (CBET)[2] was searched for all SNe with a named host galaxy discovered in the 14 yr period from 1998 January 1 to 2012 March 30. This sample was then cross-matched against the HyperLEDA galaxy data base[3] to identify all SNe for which the host galaxy had a recessional velocity (corrected for Local Group infall on Virgo) of 2000 km s^{-1} or less, corresponding to a distance limit of 28 Mpc for $H_0 = 72$ km s^{-1} Mpc^{-1}. For SNe where there was not a named host in the IAU catalogue, HyperLEDA was searched for any galaxy within 1.5 arcmin of the SN position. Finally, the coordinates of any SNe which did not have a named host or a galaxy within 1.5 arcmin and was brighter than magnitude 16 were queried via the NASA Extragalactic Database (NED).[4] We also cross-checked our sample against the catalogue of Lennarz, Altmann & Wiebusch (2012), by searching for all SNe within 35 Mpc, and manually checking the Lyon-Meudon Extragalactic Database (LEDA) for the distance to any which were not in our sample. We did not identify any SNe within our distance limit which we had missed, although we note that several SNe (e.g. SNe 2001fu, 2004ea and 2006mq) which were within our distance limit do not have an associated distance in the Lennarz et al. catalogue.

From this, we obtained a sample of 203 transients over the 14.25 yr time period within a 28 Mpc volume, as listed in Appendix A. For comparison, in Paper I we found 141 transients within the same volume over the 10.5 yr from 1998 January 1 to 2008 June 30, which appears broadly consistent with the number found here: 13.4 SNe yr^{-1} in Paper I, compared to 14.3 SNe yr^{-1} over the extended 14.25 yr period that we consider here. Most of the SNe in the sample have a spectral typing, which are listed in Appendix A together with the recessional velocity of the host. Those SNe which are of uncertain type, or which are otherwise noteworthy, and which were not discussed in Smartt et al. (2009) are discussed individually below.

(i) *SN 2010dn*

The nature of this transient is still debated. Vinkò et al. (2010) claimed that it is an eruptive outburst from a dust-enshrouded luminous blue variable (LBV), but the spectra bear resemblance to the SN2008S-like transients that are still potentially SNe (Botticella et al. 2009; Smith et al. 2009; Preito et al. 2010b). Berger (2010) set upper limits on the progenitor magnitude of SN 2010dn from archival *Spitzer* and *HST* observations of the site of the transient. Smith et al. (2011b) presented a re-analysis of the same *HST* data and similarly to Vinkò et al. favoured an SN impostor/LBV eruption as the most likely explanation. Hoffman et al. (2011) report an mid-infrared (MIR) detection of 2010dn which is again similar to that found for other SN2008S-like events. We thus leave it in the bin of 'Uncertain or non-supernova' in Table A1.

[2] http://www.cbat.eps.harvard.edu/lists/Supernovae.html
[3] http://leda.univ-lyon1.fr/
[4] http://ned.ipac.caltech.edu/

(ii) *SN 2009ip*

As noted in Table A1, the original discovery of the object we call SN2009ip was an LBV outburst. Smith et al. (2010) and Foley et al. (2011) identified the progenitor as a star of $\sim$60 $M_{\odot}$ using archival *HST* images. A similar transient, UGC 2773 OT2009-1, was discussed by Smith et al., and again was found to have a massive LBV progenitor. These LBV outbursts or eruptions are not included in our rate calculations but are listed, insofar as we are aware of their existence, in Table A1. The star which underwent an LBV eruption to give SN2009ip may now have produced an SN event, during 2012 August–September. If confirmed, this is perhaps one of the most interesting SNe ever to have occurred and is already the focus of intensive study (Levesque et al. 2012; Fraser et al. 2013; Margutti et al. 2013; Mauerhan et al. 2013; Pastorello et al. 2013; Prieto et al. 2013). The event occurred outside our timeframe; hence, we do not include it as an SN IIn for rate estimates. However, we recognize that SN 2009ip has an extremely important role in linking the progenitor star, SN explosions and the explosion mechanism.

(iii) *SN 2008iz*

The SN was discovered at radio wavelengths (Brunthaler et al. 2009) and has been the subject of extensive radio follow-up (Brunthaler et al. 2010; Marchili et al. 2010). Fraser et al. (2009) observed the SN with Gemini+NIRI (Near-Infrared Imager) and initially claimed that the SN could not be seen in the NIR. However, a careful re-analysis by Mattila et al. (2013) shows that the SN can be seen when image subtraction techniques are used. They find a likely very high line-of-sight extinction, but probably less than $A_V \approx 10$. As this was an SN which was not, and could not have been, discovered by current optical surveys, we do not consider it for our rate estimates. Its type is also currently unknown which would not enhance our measurements. It does serve as a reminder on the number of SNe that may be occurring in high star formation rate locations which are extinguished (Botticella et al. 2012; Mattila et al. 2012, 2013).

(iv) *SNe 2008ge, 2008ha, 2010ae and 2010el*

The SNe have all been identified as SN 2002cx-like. SN 2008ha is perhaps the most unusual SN considered in the sample; it showed low velocities and a faint absolute magnitude, and its interpretation is still contentious. Valenti et al. (2009) suggested that the SN was the faint core-collapse of a massive progenitor on the basis of its spectral similarity to SN 2005cs; however, Foley et al. (2009, 2010b) have questioned this interpretation and proposed that it was in fact a thermonuclear SN. Foley et al. argue that intermediate-mass elements, whose presence Valenti et al. claimed was counterfactual to a Type Ia scenario, can be present in a thermonuclear SN. Valenti et al. noted that SN 2008ha appears to be related to the class of SN 2002cx-like SNe (Li et al. 2003), and suggested that all of these may be related to Type Ibc SNe, possibly with fallback of the innermost ejecta on to the compact stellar remnant. While a fallback explosion model has been constructed for SN 2008ha (Moriya et al. 2010), it requires a progenitor which has a mass lower than that typically thought to undergo this process (Heger et al. 2003). Remarkably, three other SNe besides SN 2008ha in this sample have been suggested to be SN 2002cx-like. The discovery of this many SN 2002cx-like SNe in such a short period could suggest that a significant number of these events have gone undetected previously, likely due to their faint magnitude. For one of them, SN 2008ge, Foley et al. (2010a) have analysed pre-explosion data and found no evidence of either ongoing star formation or the young massive stellar population which would be expected to be found in the environment of a CCSN. While the nature of these SNe is still open to debate, at present the balance of evidence seems to favour a thermonuclear interpretation, and so we have excluded them from the core-collapse sample on this basis. However, given recent evidence that the class of SN 2002cx-like SNe may be significantly more heterogeneous than previously thought (Narayan et al. 2011) and may not all share the same explosion mechanism, a more detailed search for the progenitors of these SNe would be a worthwhile endeavour.

(v) *SN 2008eh*

As far as we are aware, there is no published spectrum of SN 2008eh. Hence, we have followed the lead of Horiuchi et al. (2011) and assumed that the SN is a core-collapse event (probably Type Ibc) on the basis of its absolute magnitude and light curve, and proximity to an H II region in a spiral galaxy. Nonetheless, we have excluded this SN from the rate calculations.

Table 1. The relative frequency of CCSN types discovered between 1998 and 2012.25 (14.25 yr) in galaxies with recessional velocities less than 2000 km s^{-1}, as listed in Table A1. The values in parentheses in the Number column include SNe of indeterminate subtype as discussed in the text.

SN Type	Number	Relative rate (per cent)	LOSS (per cent)
IIP	55 (70.5)	55.5 ± 6.6	$48.2^{+5.7}_{-5.6}$
IIL	3 (3.8)	3.0 ± 1.5	$6.4^{+2.9}_{-2.5}$
IIn	3 (3)	2.4 ± 1.4	$8.8^{+3.3}_{-2.9}$
IIb	12 (15.4)	12.1 ± 3.0	$10.6^{+3.6}_{-3.1}$
IIpec (87A-like)	1 (1.3)	1.0 ± 0.9	–
Ib	9 (11.4)	9.0 ± 2.7	$8.4^{+3.1}_{-2.6}$
Ic	17 (21.6)	17.0 ± 3.7	$17.6^{+4.2}_{-3.8}$
Total	100 (127)		

We summarize the relative rates of different CCSNe within our distance limit in Table A1. Discarding all SNe which were designated as Type Ia (55 SNe, or 30.2 per cent of the total classified sample) along with SN impostors and unclassified transients, we find relative rates for the various types of CCSNe as listed in Table 1 and shown in Fig. 1. SNe which were classified as a 'Type Ibc' were divided into the Type Ib and Ic bins, according to the observed ratio of these subtypes (9:17). Type II SNe were distributed between the IIP, IIL, IIb and IIp-pec bins in the ratio 55:3:12:1. Uncertainties were calculated from the standard error on a Poisson distribution (i.e. as $\sqrt{N}$). We have made no attempt to further subdivide the Type IIb SNe into the 'compact' and 'extended' subtypes proposed by Chevalier & Soderberg (2010). Although there is some scepticism as to whether these subtypes exist (Maeda 2013).

Our relative rates compare favourably with those found in Paper I, the most noticeable difference being the increase in Type IIb SNe

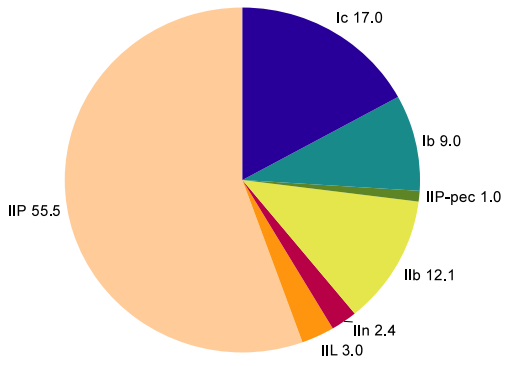

Figure 1. Percentage of CCSNe which are of a particular type as found in this work.

at the expense of Type Ibc events. A possible explanation for this is that SNe are now discovered (on average) sooner after explosion, and so Type IIb SNe which previously would have been detected late and classified as a Type Ibc are now correctly identified.

Smith et al. (2011a) measured SN rates from the Lick Observatory Supernova Search (LOSS) sample, based on those SNe selected for the luminosity function analysis by Li et al. (2011), with a total of 106 CCSNe within 60 Mpc. This is smaller than we present here, but is a much more homogeneous sample and is a well-controlled SN survey. We emphasize that we are assimilating all discoveries and not carrying out a controlled SN search, but the results should be compared given the large numbers available.

Smith et al. did not separate out the IIpec category, but did separate the Ibc-pec SNe. To facilitate a comparison between our rates, we re-distributed the Type Ibc-pec SNe from Smith et al. between the Ib and Ic categories (weighted by the Type Ib:Ic ratio), and the Type IIpec SNe from this work between the Type IIP, IIL and IIb categories. We find good agreement between the Smith rates and those presented in this paper for the Type IIb, Ib and Ic SNe. We find a Type IIP rate which is 7.3 per cent higher than that derived by Smith et al., although the uncertainties of Smith et al. and this work do overlap. If we combine the Type IIL and IIP rates, then the discrepancy is smaller, raising the possibility that some of our Type IIP SNe may in fact be Type IILs (and vice versa for Smith et al.). Smith et al. suggest that the LOSS rates are more reliable due to the SNe all coming from the same survey with well-controlled and known selection effects and good spectroscopic and photometric coverage. The latter is certainly important to distinguish between IIP and IIL SNe. In Paper I, we attempted to classify IIP SNe from literature, archive and web data searches and classified any Type II SN that had a constant magnitude phase for more than 30 d as a Type IIP. This of course is not as homogeneous a data set as that from LOSS. There are 23 SNe in common between the Smith et al. sample and that presented in Paper I (there are no extra SNe to add from 2008–2012, as the LOSS sample stops in 2006). Of those, 19 are identical classifications and two have Type II classifications by us and IIP classifications by LOSS. Including those two updated LOSS classifications here would make the IIP discrepancy worse. The other two were fairly trivial differences: Ic versus Ibc/IIb (2004ao) and Ibc versus Ib (2004qn) in Paper I and LOSS, respectively. Hence, there is no evidence we can see that points to systematic misclassifications in the smaller volume sample presented in Paper I and supplemented here.

The only SNe for which the rates and their uncertainties do not overlap at all are the Type IIn SNe, where Smith et al. find a higher rate than we do ($8.8^{+3.3}_{-2.9}$ per cent versus 2.4 ± 1.4 per cent). Smith et al. attribute this to the fact that LOSS has better and more extensive spectroscopic and photometric coverage. This is difficult to assess as the global SN community certainly has extensive resources to bear on SNe within 28 Mpc. Classification results are rapidly reported, data are published on reasonable time-scales, and we have made attempts to search archives and request private information where we can; hence, it is not clear to us that this statement in Smith et al. is necessarily correct. The Li et al. sample was produced for luminosity function work, which requires SNe to be 'in season' and full light-curve coverage from before explosion. This is essential for luminosity function measurements, but not for rate estimates. For example, long-duration plateau SNe may be preferentially excluded as their 'season' lasts longer than other types. It is still possible that the high IIn rate in LOSS is due to them being brighter and being preferentially discovered between 30 and 60 Mpc compared with <28 Mpc. However overall, the agreement is reasonable despite the differences in the construction of the two samples.

As described in Paper I for all SNe, we searched the *HST* archives using the Querator[5] and MAST[6] webpages. For CCSNe, we find that out of 127 SNe, 41 of them had *HST* images taken before discovery (i.e. 32 per cent) with the SN falling on the *HST* camera field of view (FOV). For Type Ia SNe, the fraction was 20 out of 55 (i.e. 36 per cent). Many more host galaxies of SNe had observations taken before explosion, but the SNe fell outside the small FOVs of the *HST* cameras (16 per cent of core-collapse and 16 per cent of Type Ia; see Table A1). We also searched the archives for the European Southern Observatory (ESO) telescopes,[7] Gemini North and South telescopes,[8] the Subaru Telescope,[9] the William Herschel Telescope (WHT)[10] and the Canada–France–Hawaii Telescope (CFHT)[11] for any SNe in a host with a recessional velocity of <1000 km s^{-1}. There are other 8 m class telescopes which could be of use for progenitor searches, such as the Keck telescopes and the Large Binocular Telescope; however, the absence of publicly accessible data archives precludes this.

3 ESTIMATING PROGENITOR MASSES FROM SN RATES

Smith et al. (2011a) used their observed SN rates to estimate progenitor mass ranges, given a standard initial mass function (IMF) and assuming that more massive stars will undergo greater mass-loss. They reached the conclusion that a simple single-star initial mass prescription is unable to reproduce the observed SN rates, and that binary evolution is a crucial factor for Type Ibc SNe. This is based on the relatively high rates of Ibc SNe and the fact that the mass range for classical, massive WR stars cannot reproduce the rates from Salpeter IMF arguments (also see discussion in Smartt 2009). This problem was originally noted by Podsiadlowski et al. (1992) and Nomoto, Iwamoto & Suzuki (1995), who proposed that around 30 per cent of stars above 8 $M_{\odot}$ could lose mass in interacting binaries and produce the Ibc SN population. Here we use a more detailed stellar population model to reproduce the observed rates. The main difficulty is attaching an observed SN type to the endpoint of the stellar model and the physical mass of H and He left in the model stars.

To reproduce the SN rates with a binary population, we use synthetic stellar populations from the Binary Population and Spectral Synthesis (BPASS) code. This code is able to create stellar populations of both single and binary stars, and is described in detail in Eldridge et al. (2008), Eldridge & Stanway (2009) and Eldridge, Langer & Tout (2011). In these papers, it is shown that populations including binaries are better able to reproduce observed stellar populations, both resolved and unresolved.

We have used the BPASS code to predict the relative rates of different types of SNe determined in Section 2 and listed in Table 1. Our fiducial progenitor populations are a solely single-star population and a mixed binary/single-star population with one single star for every binary. The models are computed for two metallicities,

[5] http://archive.eso.org/querator/
[6] http://archive.stsci.edu/
[7] http://archive.eso.org/cms/
[8] http://cadcwww.dao.nrc.ca/gsa/
[9] http://smoka.nao.ac.jp/
[10] http://casu.ast.cam.ac.uk/casuadc/archives/ingarch
[11] http://cadcwww.dao.nrc.ca/cfht/

$Z = 0.008$ and 0.020, corresponding to the Large Magellanic Cloud (LMC) abundance and the solar abundance, respectively. We average over these values as the SNe in our sample occur in nearby spiral galaxies which will have metallicities between these two extremes (see the discussion in Paper I). We also note that at lower metallicities quasi-homogeneous evolution may become important (Yoon, Langer & Norman 2006; Eldridge et al. 2011) but we do not currently include this pathway. We consider all stars from 5 to 120 $M_\odot$ in both single and binary populations. For the binary populations, we include a range of mass ratios for the secondary star ($q = 0.3$, 0.5, 0.7 and 0.9) and a range of initial separations from $\log(a/R_\odot) = 1$ to 4. According to our models, approximately two thirds of these binaries interact. This is consistent with the recent observations of Sana et al. (2012), although those are measurements of O stars with ZAMS masses of 20 $M_\odot$ and greater.

The precise configuration of a star at the moment of core-collapse and how this determines the resulting SN type are still quite uncertain (e.g. Heger et al. 2003; Eldridge & Tout 2004). Stellar evolution codes calculate model stars with quantitative residual envelope masses of H and He and are given SN types by assuming values of the minimum masses required to give SNe of Types II and Ib, respectively (for example, see the discussion in Dessart et al. 2011); hence, we look at this problem in a different way. We insist that the model populations must reproduce the observed relative SN rates in Table 1, as in Eldridge et al. (2011). Each star in the ensemble is evolved to the end of core-carbon burning. At this point, a resulting SN type is assigned to the model, based on the mass of the hydrogen envelope, the H-to-He mass ratio and the fraction of He in the ejecta. Then we can determine what the minimum mass of H is to produce the total numbers of Type II and Type IIP populations, respectively. As suggested by Smith et al. (2011a), we find that a single-star population cannot produce the observed rates of Ibc SNe.

A mixed population of binary and single stars (with one single star for every binary) produces end stellar points that can match the relative rates of Type Ibc versus II SNe *if* we assume that the final hydrogen and helium masses given in Table 2 are what is required to produce the various types. We find that a Type II SN requires at least 0.003 $M_\odot$ of H in the ejecta, while a Type IIP SN must have an H-to-He mass ratio of greater than 1.05 and that the total mass of hydrogen is greater than 1.5 $M_\odot$. While this mass of 0.003 $M_\odot$ of H is at first sight low, it would be the minimum for a IIb SN. The synthetic spectrum calculations of Dessart et al. (2011) show that even 0.001 $M_\odot$ can produce visible hydrogen lines (Hα in particular), as long as the surface mass fraction is higher than 0.01.

For a Type Ib SN, we require the mass fraction of helium in the ejecta to be greater than 0.61, while for a Type Ic the He fraction must be less than this. In our Ibc progenitor models, we find that the ejecta is dominated by either helium or carbon and oxygen. Therefore, for a large ejecta mass, a large mass of helium would be required for a Ib. We find few stars with such ejecta masses in the models and they all typically have a few times 0.1 $M_\odot$ of helium. Considering the typical ejecta masses for Ibc SNe of 2–3 $M_\odot$, our required ratio seems appropriate. We note that it is likely that helium mass alone does not determine if an SN is Type Ib or Ic. Other factors such as the mixing of the ejecta are important as discussed by Dessart et al. (2012).

Table 2. The required parameters for a star to give rise to a specific SN type assuming that all SN are observable.

SN type	Final mass/$M_\odot$	$M_{\rm COcore}$ /$M_\odot$	M(H) /M(He)	M(H) /$M_\odot$	M(He) /$M_{\rm ejecta}$
IIP	>2	>1.38	≥1.05	>1.5	–
II	>2	>1.38	<1.05	>0.003	–
Ib	>2	>1.38	–	≤0.003	≥0.61
Ic	>2	>1.38	–	≤0.003	<0.61

Comparing these mass values to those in Eldridge et al. (2011), which were based on the rates of Paper I, we find that they have changed by a similar percentage as the SN rates between Paper I and this paper. The most uncertain value is the amount of hydrogen that can be hidden in a Type Ibc SN, the value here being lower by a factor of 17. This difference is chiefly due to the larger fraction of Type IIb SNe in this work, which causes the minimum required H mass for a Type II SN to be lower.

We appreciate that these fairly simple and well-defined classifications of the progenitor models are, in reality, complicated by two factors. Branch et al. (2002) show that some Ib SNe may well contain some residual hydrogen, given good quality spectra and model photosphere fits. Dessart et al. (2012) discuss that it may be quite possible to get a Ic SN with helium in the progenitor star, when He I is not excited due to weak mixing of ^{56}Ni into the He-rich regions.

In summary, we can reproduce the observed rates in Section 2, with a mixed population of single stars and binaries with one single star for every binary system, as long as we attach the resulting progenitor stars into SN classification bins with the envelope mass fractions as reported in Table 2. This means that one third of all progenitors have had their envelopes stripped by binary interactions via either Roche lobe overflow or common-envelope evolution (consistent with results found in Smith et al. 2011a).

Finally, it has been suggested that SNe that form black holes directly do not produce any SN display. Heger et al. (2003) estimate that there will be no optical display if the final helium core mass is greater than 15 $M_\odot$; in our models this corresponds to a remnant mass of 8 $M_\odot$, although this idea has to be called into question by recent results from Ugliano et al. (2012). We have created a synthetic population in which we remove all core-collapse events with a remnant mass >8 $M_\odot$ (approximately 10 per cent of all SNe). Even without these events, we find that the same parameters in Table 2 can be used to reproduce the observed SN rates, so long as we increase the fraction of binaries in the population.

4 LIMITS ON TYPE IBC SN PROGENITORS FROM ARCHIVAL IMAGING

Alongside estimates from the relative rates of CCSN types, direct detections and upper limits on progenitors from archival data can help constrain their progenitor population. In the following section, we summarize the published limits for Type Ibc progenitors within a recessional velocity limit of 2000 km s^{-1}, and extend this sample with limits on an additional six SNe.

The general technique used is the same as that described in Smartt et al. (2009). We align a pre-explosion image to a post-explosion image by means of background stars in the vicinity of the SN. We then search for a source coincident with the SN in the pre-explosion image. If a coincident source is identified, then its magnitude can be measured, otherwise (as in all of the following cases) either pixel statistics or artificial star tests are used to set a limiting magnitude for a non-detection. All magnitudes quoted here are Vegamags.

4.1 2000ew

SN 2000ew was discovered by amateur astronomers (Puckett, Langoussis & Garradd 2000). The SN was initially spectroscopically

classified as a Type Ia SN (Dennefeld & Patris 2000), before Filippenko, Foley & Modjaz (2000) obtained a second spectrum which showed the SN to be of Type Ic. A Tully–Fisher distance of 18.2 Mpc has been measured for the host galaxy of SN 2000ew, NGC 3810. As the coordinates of NGC 3810 are on the outskirts of the Virgo cluster ($11^{\rm h}41^{\rm m}$, $+12^{\circ}28'$), the kinematic distance estimate (13.4 Mpc) may not be reliable. We hence adopt the Tully–Fisher distance as a more conservative estimate.

Maund & Smartt (2005) set a limit of $F606W > 24.6$ on the progenitor of SN 2000ew from pre-explosion Wide Field Planetary Camera 2 (WFPC2) imaging, while Van Dyk, Li & Filippenko (2003b) find a similar limit of $F606W > 24.7$. Maund & Smartt estimated the reddening towards the SN from nearby stars to be $E(B-V) = 0.01$, but as this is less than the foreground value from NED [$E(B-V) = 0.044$], we adopt the latter as did Maund & Smartt. The $F606W$ absolute magnitude is listed in Table 4.

Late-time NIR spectra of SN 2000ew were presented by Gerardy et al. (2002); these can help further elucidate the nature of the progenitor. Carbon monoxide (CO) emission was observed in the spectrum, albeit at a lower velocity ($\sim$2000 km s^{-1}) than might be expected for a progenitor with a 2.1 $M_{\odot}$ C+O core (Iwamoto et al. 1994). While the CO velocity could be interpreted as arising from a lower energy explosion, perhaps pointing to a less massive progenitor, it may also be explained with an asymmetric explosion with a largest component of the velocity perpendicular to the line of sight. We also note that Gerardy et al. (2002) also found narrow He I and [Fe II] lines, but no Brackett series lines, in their spectrum which they attribute to H-poor material shed by the progenitor star prior to core-collapse.

4.2 2001B

SN 2001B was discovered in IC 391 by Xu & Qiu (2001), and initially classified as a Type Ia SN by Matheson et al. (2001) before Chornock & Filippenko (2001) reclassified the SN as a probable Type Ib. A light curve was presented by Tsvetkov (2006) which reached a maximum of -17.5 in V, supporting the classification of SN 2001B as a Type Ib. IC 391 has a Tully–Fisher distance of 25.5 Mpc and a recessional velocity distance of 25.5 Mpc (from NED).

Van Dyk et al. (2003a) claimed the tentative detection of a progenitor candidate for SN 2001B from an alignment to a ground-based natural-seeing image. Subsequently, Maund & Smartt (2005) presented late-time *HST* imaging showing that the SN was offset from the candidate. Maund & Smartt set an upper limit of $F555W = 24.30 \pm 0.15$ for the progenitor of SN 2001B, which is in agreement with the limit suggested by Van Dyk et al. if their progenitor candidate was *not* the progenitor. Maund & Smartt estimate a reddening of $E(B-V) = 0.102 \pm 0.030$ from nearby supergiant stars, which is slightly lower than the line-of-sight extinction of $E(B-V) = 0.14$ from NED; we hence adopt the latter as the larger value. The absolute magnitudes are reported in Table 4.

4.3 2001ci

SN 2001ci was discovered as part of the Lick Observatory and Tenagra Observatory Supernova Searches (LOTOSS) by Swift, Li & Filippenko (2001). It was noted at discovery that the SN had a low absolute magnitude, and it was originally suggested that the transient may be an SN impostor. Filippenko & Chornock (2001) subsequently obtained a spectrum of the SN, and classified it as a highly reddened Type Ic SN, with a line-of-sight extinction of $A_V \approx 5$–6 mag.

Table 3. *HST* observational data.

	Filter	Date	Exposure time
SN2001ci			
WFPC2	*F547M*	1999-03-04	320
WFPC2	*F606W*	2001-01-21	560
WFPC2	*F658N*	1999-03-04	1200
WFPC2	*F658N*	1998-11-26	8900
WFPC2	*F814W*	1998-11-26	800
WFPC2	*F814W*	1999-03-04	140
SN2003jg			
WFPC2	*F450W*	2001-08-02	460
WFPC2	*F606W*	1994-06-21	160
WFPC2	*F814W*	2001-08-02	460
SN2004gn			
WFPC2	*F658N*	2011-03-02	1400
WFPC2	*F606W*		600
SN2005V			
ACS	*F658N*	2004-04-10	700
	F814W		120
NICMOS	*F160W*	2002-12-04	96
	F187N		640
	F190N		768
WFPC2	*F450W*	2001-07-06	460
	F814W		460
	PC *F606W*	2001-01-05	560

While NGC 3079 had been observed with *HST* prior to the SN explosion as detailed in Table 3, the images are not sufficiently deep to have a reasonable expectation of seeing a progenitor given the high extinction. In addition, we were unable to locate any high-resolution post-explosion imaging for SN 2001ci. NGC 3079 was observed with *HST*+WFPC2 in the *F300W* filter on 2001 December 9 ($\approx$6 months after the SN explosion) and the SN coordinates fall in the FOV, but it is not visible (as SNe are typically only bright at UV wavelengths for some weeks after explosion). We searched the CFHT, Gemini, Subaru, Isaac Newton Group (ING), Telescope Nazionale Galileo (TNG), and National Optical Astronomy Observatory archives, but no images of SN 2001ci were found. We have hence not considered SN 2001ci any further.

4.4 2002ap

SN 2002ap was discovered in M74 by amateur astronomers (Nakano et al. 2002), and rapidly classified as a Type Ic SN (Meikle et al. 2002). SN 2002ap was extremely energetic and bore a striking spectroscopic similarity to the 'hypernovae' 1997ef and 1998bw (Gal-Yam, Ofek & Shemmer 2002; Mazzali et al. 2002). The explosion is thought to be moderately asymmetric, both from early-time spectropolarimetry (Kawabata et al. 2002; Wang et al. 2003) and modelling of the late-time nebular spectra (Mazzali et al. 2007).

The first attempt to detect the progenitor of SN 2002ap was made by Smartt et al. (2002), who did not find a progenitor in ground-based pre-explosion imaging. A subsequent study by Crockett et al. (2007) used even deeper pre-explosion images, which still did not yield a progenitor detection. The limits for SN 2002ap remain the deepest limits for a hydrogen-deficient SN to date. The 5σ limiting magnitudes found by Crockett et al. are $B = 26.0 \pm 0.2$ mag and $R = 24.9 \pm 0.2$ mag. The limits from Smartt et al. (2002) are much shallower, with the exception of their U-band image, which

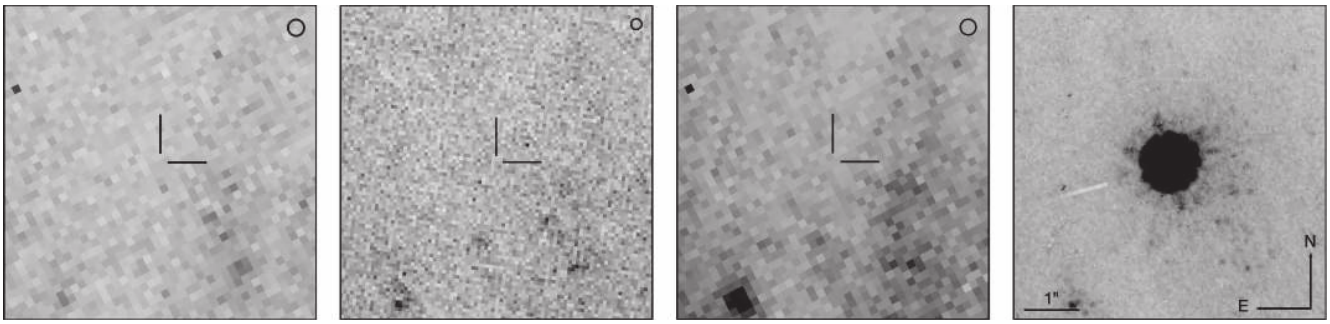

Figure 2. Pre-explosion *HST*+WFPC2 images of the site of SN 2003jg, plus a post-explosion *HST*+ACS image. Scale and orientation for each panel are identical to that indicated in the post-explosion image. The circle in the upper-right corner of each panel has a radius equal to five times the rms error in the position of the SN in that image. (a) Pre-explosion WFPC2/WF3 *F*450*W* image. (b) Pre-explosion WFPC2/PC *F*606*W* image. (c) Pre-explosion WFPC2/WF3 *F*814*W* image. (d) Post-explosion ACS/HRC *F*814*W* image.

is of interest for constraining a hot progenitor, and had a 3σ limit of 21.5 mag. Hendry et al. (2005) considered the various measurements of the distance towards the host galaxy for SN 2002ap, M74, and adopted an average value of 9.3 ± 1.8 Mpc, which we also adopt (as in Crockett et al. 2007). The total extinction (Milky Way and host galaxy) towards SN 2002ap is given by Takada-Hidai, Aoki & Zhao (2002) as $E(B-V) = 0.09 \pm 0.01$, from a high-resolution spectrum of the Na ID lines.

4.5 2003jg

SN 2003ig was discovered by LOTOSS (Graham & Li 2003), and classified by Filippenko & Chornock (2003) as a Type Ic SN approximately a week after maximum light. The SN exploded in NGC 2997, which has a Tully–Fisher distance of 12.2 ± 0.9 Mpc (Hess et al. 2009), which is in good agreement with the recessional velocity-based distance of 12.7 Mpc. The foreground extinction towards NGC 2997 from Schlegel, Finkbeiner & Davis (1998) is $E(B-V) = 0.109$ mag.

Post-explosion images of SN 2003jg were obtained in several filters with *HST*+ACS/HRC (Advanced Camera for Surveys/High Resolution Channel) on 2003 November 18. Pre-explosion WFPC2 images of NGC 2997 as detailed in Table 3 were used to search for the progenitor. The images in each filter consisted of a cr-split pair; these were combined with the CRREJ task in IRAF to reject cosmic rays. The pre-explosion WFPC2 *F*450*W* and *F*814*W* images were taken at the same pointing, with the SN position falling on the WF3 chip. To accurately identify the SN position in these, the *F*814*W* image was aligned to the post-explosion ACS/HRC *F*814*W* image. The SN position in pre-explosion *F*606*W* (on the PC chip) image was determined by aligning it to the post-explosion ACS/HRC *F*555*W* image.

20 sources were identified common to both the *F*814*W* ACS and *F*814*W* WFPC2 images, and used to derive a general transformation with an rms error of 17 mas. The SN position was measured in the ACS *F*814*W* image (j8qg10021_drz) to be (704.530, 259.953), with an uncertainty of 0.3 mas, which was transformed to the pixel coordinates of the WFPC2 *F*814*W* image (u6ea3803r_c0f), where it was found to be 246.10, 164.15, with an uncertainty of 0.2 pixels.

The pre- and post-explosion *F*606*W* WFPC and *F*555*W* ACS images were aligned with an rms error of 16 mas from a general transformation to 29 common sources; the SN position was measured in the post-explosion image to lie at pixel coordinates 704.844, 259.740 in j8qg10050_drz with an rms error of 1 mas. The SN position was transformed to the pre-explosion WFPC2 image, where it was found to have pixel coordinates on the PC chip of 334.99, 166.94 in u29r1301t_c0f, with a total uncertainty of 0.3 pixels.

Inspection of the transformed SN position in the pre-explosion frames did not reveal any coincident source, as can be seen in Fig. 2. HSTPHOT was run with a 3σ detection threshold on the pre-explosion images, but did not detect a source coincident to the SN at this significance. We calculate 5σ limiting magnitudes for the progenitor of SN 2003jg to be $F450W > 24.63$, $F606W > 24.63$ and $F814W > 23.70$ using the technique described in Crockett et al. (2011).

4.6 2004gk

SN 2004gk was discovered by Quimby et al. (2004) and classified as a Type Ic SN near maximum light. The host galaxy of SN 2004gk, IC 3311, is at an inclination angle of 90° (from LEDA), rendering any search for the progenitor optimistic at best. We note however that Elmhamdi et al. (2011) report a host galaxy extinction of $A_V = 0.372$ mag from low-resolution spectroscopy, while from photometry the SN does not appear to be heavily reddened. It is hence plausible that while IC 3311 is edge-on to our line of sight, SN 2004gk may have exploded relatively close to the edge of the galaxy. The galaxy has a negative recessional velocity as it lies within the Virgo supercluster; however, the Tully–Fisher distance to the galaxy from LEDA is ∼20 Mpc. Unfortunately, there are no pre-explosion *HST* images of the galaxy, while natural-seeing ground-based imaging is not useful at such distances. We have hence not considered SN 2004gk any further in the following.

4.7 2004gn

SN 2004gn was discovered with the Katzman Automatic Imaging Telescope (KAIT) as part of the LOSS close to the nucleus of NGC 4527 (Li, Yamaoka & Itagaki 2004). The spectral classification of SN2004gn was not reported in an IAU CBET. Private communication from the KAIT team (Cenko) confirms that it is an H-deficient SN and a Ibc classification is reasonable.[12] A Nearby Supernova Factory spectrum[13] shows it to be a Ibc similar to SN1990B at 90 d, which is a Ib. As the SN was discovered late, we cannot rule

[12] http://astro.berkeley.edu/bait/public_html/2004/sn2004gn.html
[13] http://www.rochesterastronomy.org/sn2004/sn2004gn.jpg

out that there was residual hydrogen at early times that has disappeared, but with the lack of early data we assume a classification of Ibc. We found very late time spectroscopy of the SN location from the WHT in the ING archive; however, no flux from the SN was present and so this was of no use for this work.

Besides SN 2004gn, NGC 4527 was also host to the peculiar Type Ia SN 1991T. Subsequently, the galaxy has been the subject of numerous Cepheid studies with *HST* to obtain an independent measure of the distance. The most recent of these (Saha et al. 2006) found a distance of 14.2 ± 1.3 Mpc towards NGC 4527. SN 1991T itself implies a distance of 14.1 Mpc from fits to the multicolour light curve (Jha, Riess & Kirshner 2007). We have adopted the average of these two values (14.2 ± 1.3 Mpc) as the distance towards the host. The extinction towards SN 2004gn is poorly constrained, as we have no spectra or information on phase to allow us to compare the magnitude to other Type Ibc SNe. Hence, we adopt the foreground extinction from NED, $A_V = 0.07$ mag, as a lower limit to the extinction.

Broad-band pre-explosion images for SN 2004gn (as listed in Table 3) consist of two 300 s WFPC2 *F*606*W* images, where the SN falls on the WF3 chip. Unfortunately, no post-explosion images of the SN were discovered during our archival search. As an alternative to a direct alignment between pre- and post-explosion frames, we attempted to use three isolated Sloan Digital Sky Survey (SDSS) point sources to register the combined WFPC2 WF3 image to the celestial world coordinate system (WCS). Attempting to solve this with only three sources means we are overfitting the data, and it does not make sense to quote an rms error in the alignment. However, by inspection of the positions of other SDSS sources (which were not used in determining the transformation, as they are extended), we believe that the accuracy of the registration is $\lesssim$1 arcsec.

The RA and Dec. of SN 2004gn as reported on the IAU webpages correspond to pixel coordinates of 77.8, 204.0 on the WF3 chip (using the new WCS solution). We ran HSTPHOT with a detection threshold of 3σ. Within a 1 arcsec radius of the reported SN coordinates (shown in Fig. 3), we find a single source detected above the 5σ level, at a magnitude of $F606W = 25.4$. Six other sources are detected above 3σ, but below 5σ, and with magnitudes in the range $25.4 < F606W < 25.9$. Within the larger annulus, seven sources are detected above the 5σ level, the brightest of which has a magnitude of $F606W = 24.2$. The brightest source has a large χ^2 value and a sharpness parameter which is more negative than would be expected for a single star. In fact, all of the sources detected by HSTPHOT have negative sharpness, suggesting that these are not stellar, but rather that HSTPHOT is detecting an unresolved background structure. Nevertheless, we adopt the magnitude of the brightest source detected by HSTPHOT as our limit for the progenitor magnitude, i.e. $F606W > 25.4$. The *F*658*N* images were examined, but no Hα excess was seen at the SN position.

4.8 2004gt

Monard (2004) discovered SN 2004gt in NGC 4038; the SN was spectroscopically classified as a Type Ic SN. Kinugasa, Kawakita & Yamaoka (2004) suggested that it was difficult to distinguish between the Ib and Ic subclasses; therefore, we take the conservative approach and label the SNe as Type Ibc. NGC 4038 is part of a well-studied interacting galaxy pair Arp 244, better known as the Antennae galaxies. Despite extensive observations of the Antennae, their distance is still a matter of some debate in the literature. Saviane, Hibbard & Rich (2004) derived a distance of 13.8 ± 1.7 Mpc from the tip of the red giant branch (TRGB) using *HST* WFPC2 imaging.

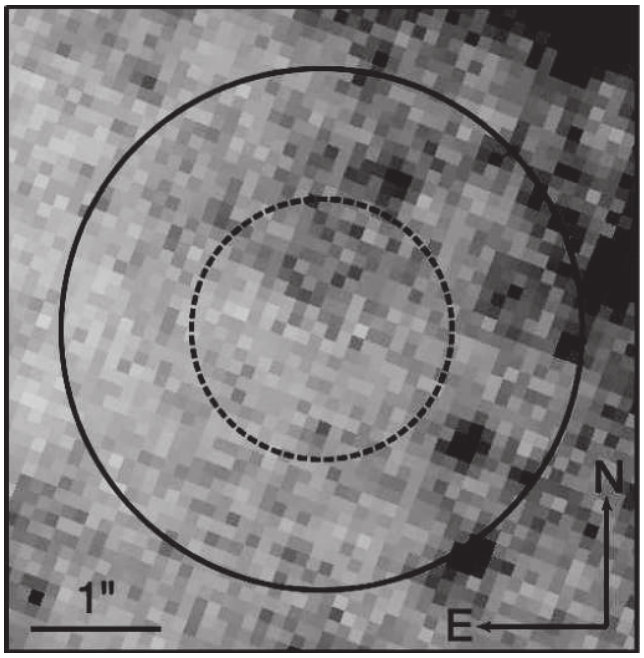

Figure 3. Pre-explosion *HST* WFPC2 image of the site of SN 2004gn, taken with the *F*606*W* filter. As no post-explosion images were available, we show a 1 arcsec (dashed line) and 2 arcsec (solid line) radius around the published coordinates for the SN.

This value was revised by Saviane et al. (2008) to 13.3 ± 1.0 Mpc, based on deeper images from *HST*+ACS. The TRGB distance is considerably closer than that expected given the recessional velocity of Arp 244, which implies a distance of ∼20 Mpc. The discovery of the Type Ia SN 2007sr in NGC 4038 provided an independent measurement of the distance from a fit to the SN light curve, yielding a value of 22.3 ± 2.8 Mpc, in disagreement with the TRGB estimate (Schweizer et al. 2008). Schweizer et al. suggest that Saviane et al. have misidentified the TRGB, and present a re-analysis of the *HST* data used by the latter which brings the TRGB distance into accord with that from SN 2007sr. We follow the suggestion of Schweizer et al. in adopting 22 ± 3 Mpc as the distance for NGC 4038, based on an average of the values from the recessional velocity, re-calibrated TRGB and SN 2007sr. The extinction towards SN 2004gt has been taken as $E(B-V) = 0.07 \pm 0.01$, following the lead of Maund et al. (2005).

Both Maund et al. (2005) and Gal-Yam et al. (2005) presented limits on the progenitor of SN 2004gt from pre-explosion *HST* images. Maund et al. found limits of $F336W > 23.04$, $F439W > 24.56$, $F555W > 25.86$ and $F814W > 24.43$. The limits found by Gal-Yam et al. are similar, but as their values are quoted in *UBVI* rather that the *HST* flight system, these cannot be compared directly. Gal-Yam et al. also present a limit from a pre-explosion Space Telescope Imaging Spectrograph image of >23.4 for the far-UV.

Using this new distance and extinction we determine upper limits for the absolute magnitudes for the progenitor of SN2004gt in Table 4.

4.9 2005V

The host galaxy of SN 2005V, NGC 2146, is a starburst galaxy and is thought to have a large population of recently formed massive stars. However, the absence of an overabundance of SN remnants may

Table 4. Properties and limits for the observed progenitors in our sample. The broad-band magnitudes with asterisks next to the value are in the standard Johnson–Cousins broad-band filters, the rest are *HST* filters with $U-F336W$, $B-F450W$, $V-F555W$, $R-F606W$ and $I-F814W$.

SN	SN type	Galaxy	Dist (Mpc)	$E(B-V)$	M_U	M_B	M_V	M_R	M_I
2000ew	Ic	NGC 3810	18.2 ± 3.3	0.04	–	–	–	−6.81	–
2001B	Ib	IC 391	25.5 ± 2.5	0.14	–	–	−8.25	–	–
2002ap	Ic	NGC 628	9.3 ± 1.8	0.09	−8.85*	−4.4*	–	−5.5*	–
2003jg	Ic	NGC 2997	12.5 ± 1.2	0.11	–	−6.30	–	−6.16	−6.99
2004gn	Ic	NGC 4527	14.2 ± 1.3	0.07	–	–	–	−5.55	–
2004gt	Ibc	NGC 4038	22 ± 3	0.07	−9.15	−7.44	−6.07	–	−7.49*
2005V	Ibc	NGC 2146	17.1 ± 3.2	0.90	–	−10.60	–	−8.80	−9.93
2007gr	Ic	NGC 1048	10.6 ± 1.3	0.08		−6.7	–	–	−8.6
2010br	Ibc	NGC 4051	12.7 ± 2.0	0.04	–	–	–	−4.92	–
2011am	Ib	NGC 4219	24.5 ± 5.6	0.60	–	–	–	−7.44	–
2011hp	Ic	NGC 4219	24.5 ± 5.6	0.50	–	–	–	−7.46	–
2012au	Ib	NGC 4790	23.6 ± 2.0	0.04	–	−8.0	–	−7.5	−8.6

indicate that the starburst is at an earlier stage than similar galaxies such as M82 (Tarchi et al. 2000). The kinematic and Tully–Fisher estimates for the distance towards NGC 2146 agree well (17.2 and 16.9 Mpc, respectively); however, the sosies estimate is significantly larger at 27.7 Mpc. As NGC 2146 appears to have a slightly irregular morphology, it is possible that the sosies method is not a reliable measure in this case. We have hence discarded this measure, and adopted the mean of the kinematic and Tully–Fisher distances.

Mattila et al. (2005) discovered SN 2005V in the near-infrared, although the early-time $J-H$ and $H-K$ colours of the SN do not support very high levels of extinction. Mattila et al. find $J-H=0.1$ mag, $H-K=0.2$ mag for SN 2005V, which is indistinguishable from the typical $J-H$ and $H-K$ colours of Ibc SNe (Hunter et al. 2009). Taubenberger et al. (2005) classified the SN as a Type Ibc, but with a strong Na ID absorption [equivalent width (EW) = 5.5 Å] and a red continuum which does indicate significant reddening. Unfortunately, there is no published photometry of SN 2005V, so we cannot compare the optical colours and absolute magnitude to other Type Ibc SNe. Using the relation of Turatto, Benetti & Cappellaro (2003) between NaD absorption and reddening, we infer $E(B-V)\sim 0.9$; however, we are somewhat sceptical of the veracity of this estimate due to the large scatter in the relation (Poznanski et al. 2011). Nonetheless, we adopt $E(B-V)$ as the conservative option, as an *over*estimate of A_V will only serve to make our limits *less* restrictive. On a more qualitative level, we also note that the SN is close to the nucleus of the galaxy, that a large number of dust lanes are seen in the *HST* images and that the SN position is offset by ∼0.15 arcsec from one of these lanes.

Pre-explosion WFPC2 images as listed in Table 3 were downloaded from the *HST* archive. Cr-split pairs were combined with CRREJ to remove cosmic rays. The SN position lies on the PC chip in the $F606W$ image, and on the WF3 chip in the $F450W$ and $F814W$ filter images, as shown in Fig. 4. To identity the SN position in the pre-explosion images, we used images of the SN obtained with the ACS/HRC on 2005-08-08.

The $F606W$ pre-explosion was aligned to the $F555W$ post-explosion image. 26 sources were used to fit a general transformation with an rms error of 0.164 WFPC2/PC pixels, corresponding to 8 mas. The SN position was measured in j90n04020_drz to be 578.770, 609.971 with an error of $\ll 1$ mas. The SN position was transformed to the pre-explosion image, where it was found to have pixel coordinates 331.27, 411.27 in u67n1801r_c0f.fits, with an uncertainty of 0.16 pixels. HSTPHOT did not detect a coincident source at the 3σ level, and we calculated the limiting 5σ magnitude as before to be $F606W > 24.76$.

The $F814W$ pre-explosion image was aligned to the post-explosion $F814W$ image with 17 sources, for an rms error of 0.17 WFPC2/WF pixels, or 17 mas. The SN position was measured in the ACS/HRC $F814W$ image to an accuracy of 1.5 mas, and transformed to the pre-explosion WFPC2 $F814W$ image. We derived transformed coordinates of 140.19, 94.01 for the SN in u6ea2803r_c0f. No source was evident at the SN location, and HSTPHOT detected no source at the 3σ level or above in either the $F450W$ or $F814W$ images. We calculate 5σ limiting magnitudes for the progenitor of SN 2005V of $F814W > 22.80$, $F450W > 24.05$.

The ACS pre-explosion images were also examined. The $F814W$ image showed no source coincident with the SN, and as the limit is comparable to that from the WFPC2 $F814W$ image, this was not considered any further. The $F658N$ image (narrow-band Hα) showed flux at the SN position, but as there were no corresponding continuum observations, it was unclear whether this flux comes from Hα emission or was simply from the high-background levels. The Near Infrared Camera and Multi-Object Spectrometer (NICMOS) data were taken with the NIC3 camera, which has a pixel scale of 0.2 arcsec. The narrow-band images were not examined in detail, while the broad-band $F160W$ image was too shallow to be of use, especially for constraining a compact (and presumably hot) progenitor.

4.10 2005at

SN 2005at exploded in NGC 6744, at a distance of 14.1 ± 2.8 Mpc. Unfortunately, the SN suffers from a high level of extinction ($A_V\sim 2.3\pm 0.3$; Kankare, private communication), while the pre-explosion data consist of ground-based Very Large Telescope imaging (VLT+FORS, VIMOS, ISAAC and the ESO 2.2 m+WFI) rather than from *HST*. Using the ESO exposure time calculators,[14] we estimated 5σ limiting magnitudes for the pre-explosion images, and took these together with the distance modulus and extinction $A_V\sim 2.3$ to estimate the absolute magnitude reached be the pre-explosion data. As the absolute magnitude reached is between −9 and −11 mag, which is between 1.5 and 3.5 mag brighter than the most luminous WR star in Fig. 8, these are of no use for constraining the progenitor. Furthermore, late-time images of NGC 6744

[14] http://www.eso.org/observing/etc/

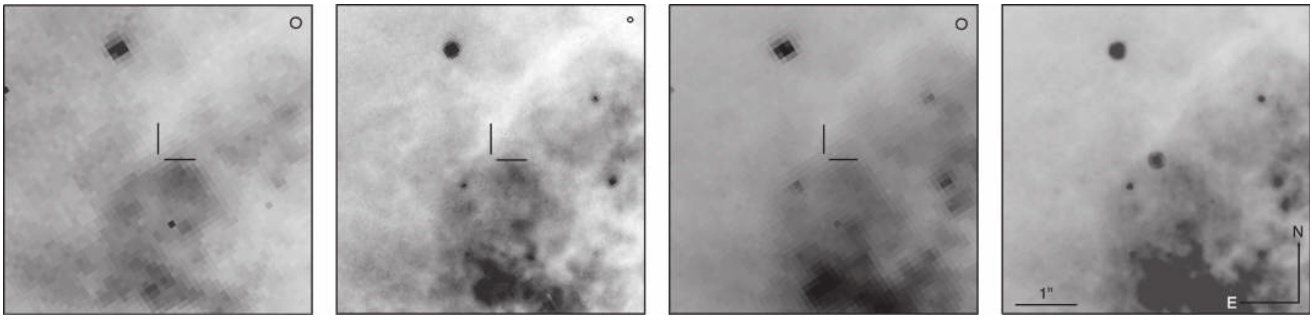

Figure 4. Pre-explosion *HST*+WFPC2 images of the site of SN 2005V, plus a post-explosion *HST*+ACS image. Each panel covers a 5 arcsec ×5 arcsec region. Scale and orientation for each panel are identical to that indicated in the post-explosion image. (a) Pre-explosion WFPC2/WF3 *F*450*W* image. (b) Pre-explosion WFPC2/PC *F*606*W* image. (c) Pre-explosion WFPC2/WF3 *F*814*W* image. (d) Post-explosion ACS/HRC *F*814*W* image.

obtained in 2012, when subtracted from the pre-explosion images, show no sign of a progenitor disappearance (Kankare, private communication). We have hence not considered SN 2005at any further in this work.

4.11 2007gr

SN 2007gr is a Type Ic SN which exploded in NGC 1058; the SN was first discovered by Madison & Li (2007), and spectroscopically classified by Chornock et al. (2007). The photometric evolution of SN 2007gr was similar to that of SN 2002ap (Hunter et al. 2009), but with marked spectroscopic differences. Where the spectra of SN 2002ap resembled those of the broad-lined Ic 1998bw, SN 2007gr is spectroscopically similar to a prototypical Type Ic such as SN 1994I. The spectra of SN 2007gr were also notable for the presence of strong carbon absorption (Valenti et al. 2008b). Modelling of late-time nebular spectra for SN 2007gr (Mazzali et al. 2010) suggests an ejected oxygen mass of 0.8 $M_\odot$, which implies that the CO core that exploded resulted from a star with ZAMS mass ∼15 $M_\odot$. Such a progenitor would not have been massive enough to lose its H and He envelopes through stellar winds, and so must have been stripped as part of a binary system.

It was claimed by Paragi et al. (2010) from radio interferometry that SN 2007gr was expanding at relativistic velocities. Together with the absence of extremely high velocities in optical spectra, and the polarization seen in spectropolarimetry (Tanaka et al. 2008), Paragi et al. explained the properties of SN 2007gr with a small amount of material in a low-energy, bipolar jet (seen in radio), coupled with mildly aspherical, non-relativistic ejecta. However, this interpretation was questioned by Soderberg et al. (2010), who claimed from X-ray and radio data that they could fit the evolution of the SN at these wavelengths with a non-relativistic ejecta.

Crockett et al. (2008) used pre-explosion *HST* and post-explosion Gemini images to show that the SN exploded on the edge of what appears to be either a small compact cluster or a bright supergiant star. Assuming it to be a cluster and fitting of the cluster age yielded uncertain results; STARBURST99 models give an age of 7 ± 0.5 or 16–21 Myr with progenitor masses of 28 ± 4 and 14–11 $M_\odot$, respectively (Crockett et al. 2008). Regardless of whether the nearby source is a star or a cluster, Crockett et al. (2008) estimated detection limits for an unseen, point-like progenitor: $F450W > 23.7$ and $F814W > 21.7$. These are not as deep as typical *HST* WFPC2 images due to the proximity of the SN to this bright object. Assuming $E(B-V) = 0.08$ and a distance of 10.6 Mpc as adopted in Crockett et al. (2008), this corresponds to absolute magnitude limits for the unseen progenitor of $F450W > -6.7$ and $F814W > -8.6$.

4.12 2010br

SN 2010br was discovered in NGC 4051 by amateur astronomers (Nevski et al. 2010) and spectroscopically classified as a Type Ibc SN (Maxwell et al. 2010). NGC 4051 has a recessional velocity distance of 12.7 Mpc (via NED) and a Tully–Fisher distance of 12.2 Mpc (Tully et al. 2009). We adopt the average of these two values, 12.5 ± 0.3 Mpc, as the distance to NGC 4051. The foreground extinction towards SN 2010br is $A_V = 0.04$ mag, from NED, which we adopt as a lower limit to the extinction.

HST pre-explosion imaging consisted of a single WFPC2 *F*606*W* image taken on 1994 June 06 (u2e64a01t_c0f). Unfortunately, the image was not taken as a cr-split pair, so we have been careful to ensure that there are no cosmic rays in the image at the position of SN 2010br. The SN fell on the PC chip, and so we aligned the PC chip only to a 2340 s post-explosion image taken in the *F*547*M* filter with WFC3 on 2010 July 17. Using 16 sources we obtained an rms error of 0.2 pixels (10 mas) in a general fit. The SN position was measured in the post-explosion image (ib5e04010_drz) to be 2002.08, 2067.76, with an rms error of $\ll$1 mas. The SN position was transformed to the pre-explosion image, where it was found to be 670.77, 724.56 on the PC chip. We show the images in Fig. 5.

No source was detected by HSTPHOT when it was run on the pre-explosion image with a 3σ threshold. Using the same method as previous, we calculate a limiting magnitude of $F606W > 25.7$ for the progenitor of SN 2010br.

4.13 2011am

Bock, Parker & Brimacombe (2011) discovered SN 2011am in NGC 4219, and Morrell, Stritzinger & Ho (2011) classified the SN shortly after as a young Type Ib SN. Morrell et al. noted the presence of strong Na ID absorption at the redshift of the host, suggesting significant extinction. Tully et al. (2009) give a Tully–Fisher distance for the host of 21.0, while the kinematic distance from NED (corrected for infall on Virgo, GA and Shapely) is 22.5 Mpc. We adopt the Tully–Fisher distance.

Pre-explosion imaging of the site of SN 2011am consists of a 600 s WFPC2 exposure in the *F*606*W* filter, obtained on 1996 March 16. The SN position lies close to the edge of the PC chip. We attempted to obtain an adaptive optics (AO) image of SN 2011am

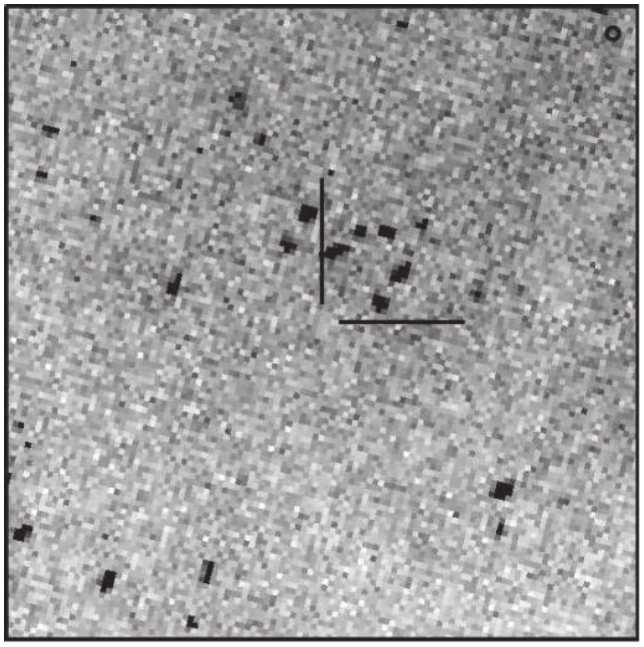

Figure 5. Pre-explosion *HST*+WFPC2 image of the site of SN 2010br, plus post-explosion *HST*+WFC3 image. Each panel covers a 5 arcsec × 5 arcsec region. Scale and orientation for each panel are identical to that indicated in the post-explosion image; the circle in the upper right corresponds to five times the positional rms error. (a) Pre-explosion WFPC2/PC *F*606*W* image. (b) Post-explosion WFC3 *F*547*M* image.

with the VLT+NaCo; however, the correction obtained was unsatisfactory due to poor conditions at the time of the observations. Instead, we used an *R*-band image obtained of SN 2011am on 2011 March 27 with the New Technology Telescope, NTT+EFOSC2, under good (∼0.8 arcsec) seeing conditions to identify the progenitor. The EFOSC2 image was aligned to a pre-explosion Hubble

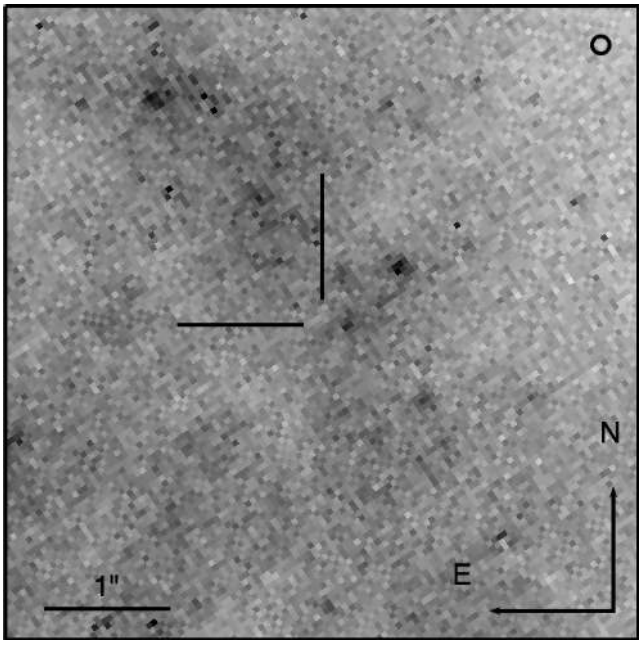

Figure 6. Pre-explosion *HST*+WFPC2 image of the site of SN 2011am. The panel covers a 5 arcsec × 5 arcsec region; scale and orientation are as indicated. The circle in the upper right corresponds to the positional rms error.

Legacy Archive[15] (HLA) mosaic (u3321601b_drz.fits) to an accuracy of 75 mas. The HLA mosaic was then in turn aligned to the PC chip image, where the transformed SN position was found to be 724.10, 355.78, with an uncertainty of 76 mas.

As shown in Fig. 6 SN 2011am is close to (but probably not coincident with) a source with $F606W = 24.204 \pm 0.003$. This source is also classified by HSTPHOT as extended. The formal 5σ limit for the progenitor is 25.8 mag. The extinction towards SN2011am is uncertain but is almost certainly significant. The spectrum at around −6 d from Morrell et al. is significantly redder than that of SN2007Y at a similar epoch (−7 d from Stritzinger et al. 2009). We dereddened the spectrum of SN2007Y by $E(B-V) = 0.112$ as estimated by Stritzinger et al. (2009), and dereddened the spectrum of SN2011am to match the blue continuum of SN2007Y, finding a very good match with $E(B-V) = 0.6 \pm 0.1$. The intermediate-resolution spectrum of Morrell et al. nicely resolves the Na D1 and D2 lines in the Milky Way and NGC 4219. The Milky Way components' EWs for D1 (5897 Å) and D2 (5891 Å) are 0.34 and 0.39 Å, respectively. Using the Poznanski, Prochaska & Bloom (2012) relation this suggests $E(B-V) = 0.1 \pm 0.02$, which is in reasonable agreement with the dust map line-of-sight estimate of Schlegel et al. (1998) $E(B-V) = 0.13$. However, there is very strong absorption in the ISM of NGC 4219, giving EWs for D1 (5897 Å) and D2 (5891 Å) of 0.86 and 1.26 Å. The Poznanski et al. (2012) relation saturates at EWs of around 0.7 Å, and hence cannot be reliably used and we note that applying it would give values of $E(B-V) = 2.3$ and 6.5, both of which would give unphysical blue spectral slopes and unrealistic absolute magnitudes. Hence, we adopt $E(B-V) = 0.6 \pm 0.1$. The corresponding absolute magnitude is given in Table 4.

[15] http://hla.stsci.edu/

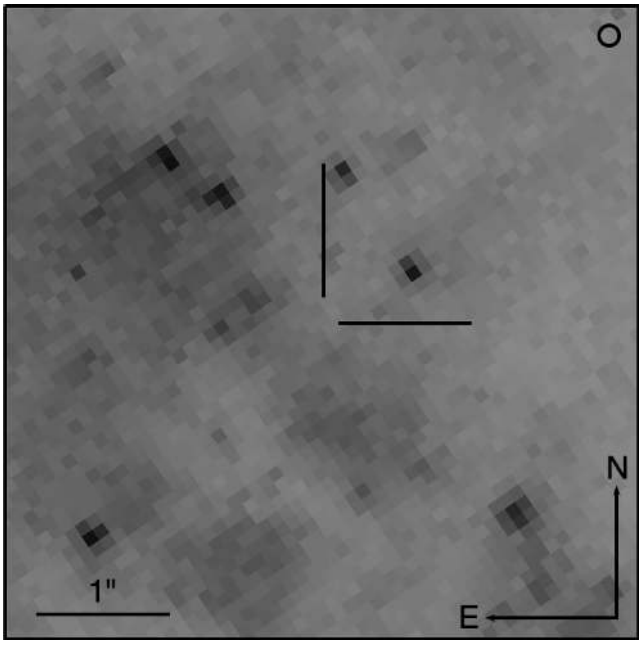

Figure 7. Pre-explosion *HST*+WFPC2 image of the site of SN 2011hp. The panel covers a 5 arcsec × 5 arcsec region; scale and orientation are as indicated. The circle in the upper right corresponds to the positional rms error.

4.14 2011hp

SN 2011hp exploded in the same galaxy as SN 2011am, and so we adopt the same distance of 21.0 Mpc (Tully et al. 2009). The SN was first discovered by Monard, Stritzinger & Foley (2011), and classified by Strizinger & Foley (2011) as a Type Ic SN discovered around maximum light. Fraser et al. (2011) reported a limit for the progenitor of $F606W > 26$.

The pre-explosion image for SN 2011hp is the same as that used for SN 2011am. Unfortunately, we have no high-resolution imaging for SN 2011hp, and so we are forced to rely on the same natural-seeing image as used by Fraser et al. (2011) for a progenitor identification. We confirm the position measured by Fraser et al. in the mosaic of all four WFPC2 detectors, where the SN falls on the WF4 chip, as shown in Fig. 7. However, we find a shallower limit than that reported by Fraser et al., and calculate a new 5σ limit for the progenitor of SN 2011hp of $F606W > 25.5$.

The spectra of 2011hp are also redder than normal, indicating significant line-of-sight extinction similar to SN 2011am. We used a spectrum from the ESO programme 184.D-1140 with EFOSC2 on the NTT (3500–9000 Å, resolution 17.7 Å) taken at +15 d after peak (Elias-Rosa et al., in preparation) to compare with the low-extinction Type Ic 2007gr. The spectrum of 2011hp needs to be dereddened by $E(B-V) \simeq 0.5$ to match the spectral shape of 2007gr [when it is dereddened by $E(B-V) = 0.092$]. Hence, we adopt $E(B-V) = 0.5$, resulting in the absolute magnitude limit reported in Table 4.

4.15 2012au

SN 2012au was identified in the Catalina Sky Survey, and subsequently classified as a Type Ib SN (Silverman et al. 2012). The host galaxy, NGC 4790, has a recessional velocity distance (Virgo corrected) of 21.8 Mpc and a Tully–Fisher distance of 23.6 Mpc (both from NED). We adopt the latter, corresponding to $\mu = 31.9$, and a foreground extinction of $A_V = 0.13$. Pre-explosion imaging consists of 2 × 160 s images in each of *F*450*W*, *F*606*W* and *F*814*W*, taken with *HST*+WFPC2. We did not obtain an AO image of SN 2012au; however, Van Dyk et al. (2012) set 3σ upper limits of $F450W > 24.8$, $F606W > 25.8$ and $F814W > 25.1$ from an alignment with a natural-seeing image. Van Dyk et al. also identified a source slightly outside the transformed SN position (offset by 0.2 arcsec) in the *F*450*W* filter image, with a magnitude of $F450W = 24.4$. This corresponds to an absolute magnitude in *B* of −7.2 mag. We have re-estimated the limiting magnitudes in these images at the position of the SN and find significantly brighter limiting magnitudes, due to the very high sky background in this vicinity. We determine 5σ limiting magnitudes of $F814W > 23.4$, $F606W > 24.5$ and $F450W > 24.1$.

5 LIMITS FOR THE SAMPLE

Table 4 contains the detection limits for 12 hydrogen-deficient CCSNe. We have not listed metallicity information for these progenitors due to the lack of homogeneous measurements for the host galaxies. However, all the hosts are large spiral galaxies and therefore are expected to have metallicities in the range between that of the Magellanic Clouds and the Milky Way (see the discussion in Smartt et al. 2009). Distances in Table 4 are as discussed in the text. To gain insight into the progenitors of Type Ibc SNe, we compare our observed limits to a number of different plausible progenitor populations.

5.1 Limits on progenitors from the observed WR star population

A reasonable hypothesis is that the Type Ibc SNe come from massive WR stars. These are stars which will produce Fe cores and have atmospheres devoid of hydrogen and helium (the WN and WC+WO stars, respectively). The classical WR stars are thought to arise in very massive stars that lose their envelopes through stellar winds, potentially enhanced by binary interaction and stellar rotation. These stars appear to be in clusters with turn-off masses that imply lower limits of $>25\,M_{\odot}$ in the Milky Way and Magellanic Clouds (Massey 2003; Crowther 2007). Due to their high temperatures and high mass-loss rates, the WR stellar radii, masses and bolometric corrections are highly variable. With the strong emission line spectra, this leads to a large range in the absolute magnitudes of the stars. Hence, there is no easy way to set meaningful luminosity or mass limits, as can be done for non-detections of IIP progenitor stars (e.g. Smartt et al. 2003; Van Dyk et al. 2003a) and we need a simpler comparison method. If we assume that this population of stars is responsible for the Type Ibc SNe that we see locally, we can test if our non-detections are significant. In other words, what is the probability that we have not detected a progenitor star simply by chance? Of course, this assumes that the WR stars that we observe now do not change their optical fluxes significantly before core-collapse, and we discuss this debatable point below.

We compare our limits to the observed magnitude distribution of WR stars in the LMC. Massey (2002) presented a catalogue of *UBVR* photometry for stars in the LMC, and used the WR catalogue of Breysacher, Azzopardi & Testor (1999) to report broadband magnitudes for isolated WR stars. This is reasonably complete, and covers a large range of WR luminosities and optical magnitudes. As the catalogue of Massey contains *BVR* magnitudes for WR stars (whereas most of our progenitor limits are in the *HST F*450*W*, *F*555*W* and *F*814*W* filters), we have calculated *HST* Johnson–Cousins colours for each of the WR spectral types, and

Table 5. Adopted temperature scale for WR types, together with colours from synthetic photometry of Potsdam models. For each colour, the two values listed are the colour as calculated from the model at that temperature with the smallest and largest transformed radii/mass-loss rates, respectively.

WR type	Models ($R_{\rm min}$ to $R_{\rm max}$)	$T_{\rm eff}$ (kK)	$F450W-B$	$F555W-V$	$F606W-R$	$F814W-I$
WN9	03-10 to 03-04	30	0.026 to 0.042	−0.043 to −0.018	−0.047 to −0.090	−0.102 to −0.090
WN8	04-15 to 04-04	35	0.000 to 0.041	−0.074 to −0.022	0.016 to −0.086	−0.127 to −0.085
WN7	05-16 to 05-04	40	−0.002 to 0.041	−0.081 to −0.030	0.020 to −0.090	−0.123 to −0.081
WN6	07-18 to 07-04	50	−0.006 to 0.047	−0.090 to −0.032	0.024 to −0.092	−0.113 to −0.083
WN5	09-20 to 09-04	60	0.004 to 0.051	−0.074 to −0.029	0.035 to −0.094	−0.119 to −0.044
WN4	11-21 to 11-06	75	0.003 to 0.045	−0.088 to −0.038	0.019 to −0.096	−0.078 to −0.042
WN3	13-21 to 13-08	100	−0.001 to 0.039	−0.133 to −0.040	−0.010 to −0.086	−0.079 to −0.026
WN2	17-21 to 17-12	150	−0.069 to 0.037	−0.207 to −0.042	−0.030 to −0.080	−0.139 to −0.025
WN1	18-21 to 18-13	180	−0.083 to 0.032	−0.226 to −0.043	−0.031 to −0.076	−0.096 to −0.023
WN	Mid-range		−0.016	−0.122	−0.030	−0.162
WC5	11-18 to 11-06	80	0.041 to 0.045	−0.059 to −0.034	0.001 to −0.095	−0.879 to −0.875
WC4	15-22 to 15-09	120	0.010 to 0.040	−0.099 to −0.042	0.019 to −0.121	−0.712 to −0.648
WC	Mid-range		0.028	−0.071	−0.051	−0.764
WO3	19-26 to 19-24	200	0.004 to −0.064	−0.102 to −0.204	0.037 to 0.168	−0.727 to −0.667
WO	Mid-range		−0.03	−0.153	0.103	−0.697

used these to convert the *BVR* magnitudes in the Massey (2002) catalogue to the *HST* filter system.

We first fitted a function of form $Ax + B$ to the effective temperatures of a sample of Galactic WR stars from Hamann, Gräfener & Liermann (2006) of spectral type WN*x*, where A and B are fitting coefficients. As there were no WN1 stars in the sample of Hamann et al. (2006), we have assumed a temperature of 180 kK for this subtype. From this fit, we have estimated a temperature for each of the WN spectral types, as listed in Table 5. Temperatures for the WO and WC stars were taken from Sander, Hamann & Todt (2012). We then downloaded model WR spectra from the Potsdam data base (Hamann & Gräfener 2004),[16] appropriate to the temperature of each WR subtype. Models were available for a range of transformed radii (effectively a range of mass-loss rates) at each temperature; we have taken the models with the largest and smallest transformed radii as the extreme cases. For each model, we used the IRAF.SYNPHOT package to perform synthetic photometry on the flux-calibrated model spectrum, and from this calculate a colour as listed in Table 5.

Along with spectral type, the colours of the WR stars depend strongly on radius, as the emission lines which dominate WR spectra are stronger in more compact models. The emission line strength will also depend on the wind velocity of the WR star. As these are largely unquantified uncertainties, we will simply adopt average $F450W-B$, $F555W-V$ and $F606W-R$ colours for each of the WN, WC and WO types, as listed in Table 5.

We plot the observed sample of WR stars in Fig. 8 along with the limits from our progenitor sample in each of the $F450W$, $F555W$ and $F606W$ filters.

It is trivial to calculate the probability of not detecting any Type Ibc progenitor thus far, assuming that they are randomly drawn from the population of WR stars shown in Fig. 8. For each progenitor with a limit in B, V or R listed in Table 4, we count the number of WR stars with a magnitude brighter than this limit. For most of our Type Ibc SN sample, less than ∼10 per cent of WR stars are brighter than our limit (and hence can be ruled out). We can then calculate the probability of not detecting *any* Type Ibc progenitors to date as $P = \Pi(1 - F_n)$, where F_n is the fraction of WR stars brighter than a particular Type Ibc SN progenitor limit. Using all the limits in Table 4, we find a probability of only 15 per cent that we would not have seen a Type Ibc progenitor thus far.

The WR stars in the LMC which are plotted in Fig. 8 are a mix of massive binaries and single stars, while it is of course a single star that explodes. However, this does not matter for our test, as if the typical WR population of the LMC were giving rise to Type Ibc SNe we should see the progenitor stars or their binary systems.

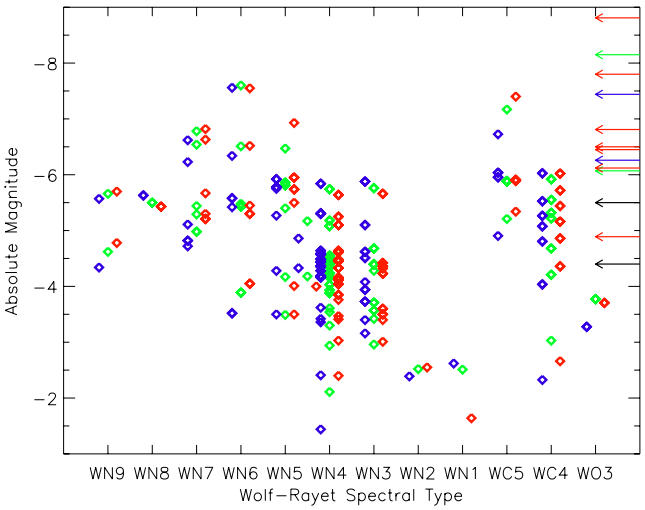

Figure 8. Limiting magnitudes for the progenitors of Type Ibc SNe (indicated with arrows), compared to the observed magnitudes of LMC WR stars from Massey (2002). WR star magnitudes have been converted to $F450W$, $F555W$ and $F606W$ (indicated by blue, green and red diamonds or arrows) as described in the text, and corrected for foreground extinction [$E(B - V) = 0.080$] and the distance of the LMC (μ − 18.50 mag). All progenitor limits are in the *HST* filters, with the exception of those for SN 2002ap, which are in the Johnson–Cousins filter system.

[16] http://www.astro.physik.uni-potsdam.de/∼wrh/PoWR

Table 6. The probabilities that no progenitor would have been observed given the different model populations.

			Progenitor models			
SN	SN type	Observed WRs	Single WR stars	Single Post-He burn	Binary WR stars	Binary Post-He burn
2000ew	Ic	0.96	1.00	1.00	0.93	0.94
2001B	Ib	1.00	1.00	1.00	1.00	1.00
2003jg	Ibc	0.94	1.00	1.00	0.86	0.89
2004gt	Ibc	0.94	0.98	0.99	0.83	0.87
2005V	Ibc	0.99	1.00	1.00	1.00	1.00
2007gr	Ic	0.97	1.00	1.00	0.90	0.92
2011am	Ib	0.99	1.00	1.00	0.97	0.97
2011hp	Ib	0.99	1.00	1.00	0.97	0.97
2012au	Ib	0.99	1.00	1.00	0.97	0.98
2002ap	Ic	0.48	0.089	0.18	0.21	0.35
2004gn	Ic	0.76	0.95	0.99	0.77	0.82
2010br	Ibc	0.57	0.62	0.73	0.55	0.66
Model probability		0.16	0.051	0.13	0.048	0.12
02ap, 04gn, 10br only		0.21	0.052	0.13	0.089	0.19

We have performed a similar probability calculation for the sample of WR stars described by Bibby & Crowther (2010, 2012). Here their sample is biased towards brighter magnitudes with no stars in their sample below $M_V \simeq -4$. If we assume that this is representative of the progenitor population, then the probabilities in Table 6 decrease. For example, our most restrictive event SN 2002ap would have a probability of 0.01. The probability for the entire population would be 4×10^{-6} and so essentially zero, even without this SN. This demonstrates how difficult it is to detect WR stars in other galaxies at great distances let alone progenitors that may also be fainter than these WR stars. It also demonstrates that this bright end of the WR luminosity function is almost certainly not producing the Ibc SNe that we see in the local Universe.

5.2 Limits on progenitors from population modelling

Comparing the progenitor limits from archival imaging to the observed population of WR stars is the simplest approach to constraining the progenitor population of Type Ibc SNe. However, it is limited by the fact that observed WR stars will lie within a range of different evolutionary states, with some stars closer to core-collapse than others. It is possible that Type Ibc progenitors become fainter in optical bands as they evolve closer to the point of core-collapse (e.g. Yoon et al. 2012). To account for this, we compare our observed progenitor limits to synthetic progenitor populations created with BPASS.

There is great uncertainty in creating models of WR stars, both in atmosphere and stellar models. A great amount of work has been performed recently improving the models of WR atmospheres (e.g. Sander et al. 2012); however, uncertainties still remain. Numerical models of WR stars have also improved; however, there are still ambiguities, mainly concerning the mass-loss rates of these stars. Comparing our models to those of Yoon et al. (2012) and Ekström et al. (2012) we find that the evolution is qualitatively similar. There is different evolution however towards the endpoints of the models. In Ekström et al. (2012) most WR models increase in effective temperature up until core-collapse and so become optically fainter. The difference is most obvious for more massive WR stars. This difference is likely to be due to Ekström et al. (2012) adopting a lower solar metallicity and different mass-loss rates. Those of Yoon et al. (2012) and our models both have effective temperatures that decrease slightly towards the end of evolution. But the models of Yoon et al. (2012) also reach higher surface temperatures than our models. We assume this to be the result of the models of Yoon et al. (2012) starting on the helium main sequence while our models arise naturally due to binary evolution so typically experience less mass-loss. The difference could also be due to how the different stellar evolution codes deal with the WR inflation effect as discussed by Petrovic, Pols & Langer (2006) and Gräfener, Owocki & Vink (2012). This is perhaps the key question that must be resolved before we are able to accurately predict the pre-SN structure and parameters for WR stars. We do not use the final endpoints of our models to estimate progenitor luminosities because of the question of whether or not progenitors are inflated. Inflation refers to the increase in the radii of stellar models due to radiation pressure on the iron bump in the stellar opacity (Ishii, Ueno & Kato 1999). The occurrence has been shown to depend on metallicity and mass-loss rates used in the stellar models (Petrovic et al. 2006). The difference in radii caused by this effect will also affect the effective temperatures of the models. Our method includes a range of radii for each model in the population therefore allowing, in an approximate way, for the uncertainty in WR stars' radii.

It is difficult to determine how WR stars do evolve towards the end of their lives and therefore we take this into consideration in our analysis below. We stress that while there are many uncertainties in predicting the WR population, our BPASS synthetic populations have been tested against a number observations where the modelling of WR stars is key to reproducing the observations from nearby to high redshift (e.g. Eldridge et al. 2008; Eldridge 2009; Eldridge & Stanway 2009, 2012). To provide further validity to our WR models in Fig. 9, we compare the locations predicted for our single-star and binary population in the Hertzsprung–Russell (HR) diagram to those inferred from the Potsdam models for observed WR stars in Hamann et al. (2006) and Sander et al. (2012). The figure shows that in general our models when hydrogen-free do match the location of observed WR stars. We note that the observed sample has complex selection effects and does not represent a constant star formation history or fully sampled IMF. Therefore, our model population can only be compared to the region of the WR stars on the HR diagram, and not their relative distribution. We have also assumed that a model

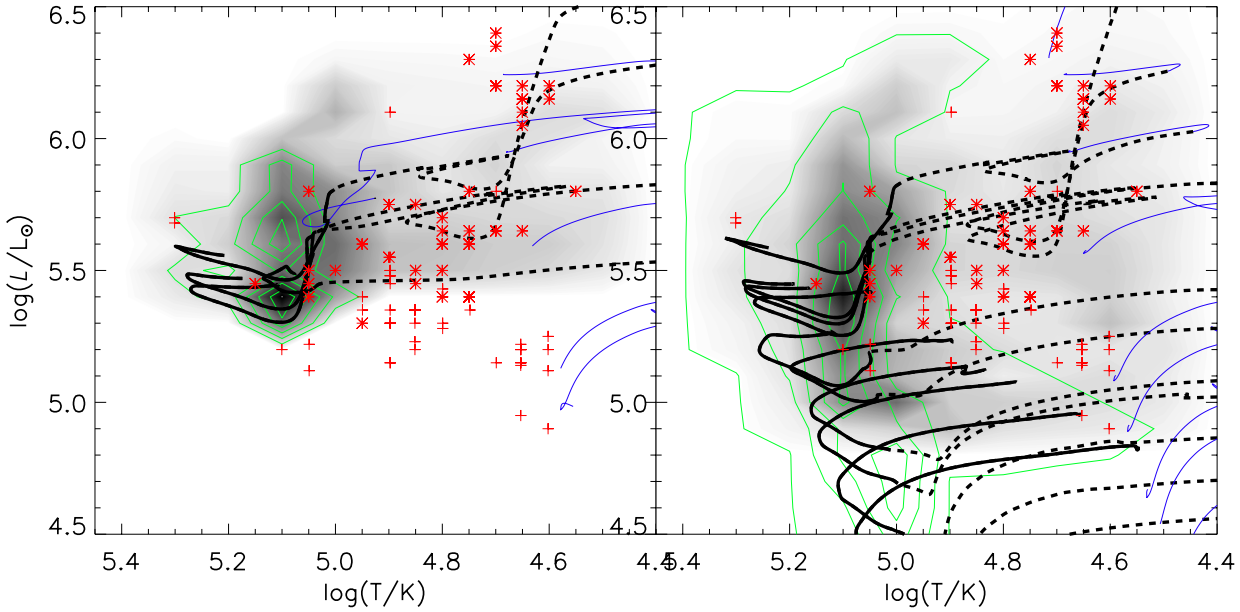

Figure 9. Theoretical HR diagrams that compare models and observations of WR stars. The shaded regions show the density of the population we expect from a synthetic population of the WR stars calculated by BPASS assuming constant star formation, a Salpeter IMF and requiring that $\log(L_{\rm WR}) > 4.9$. Helium stars less luminous than this still contribute to SNe but are assumed not to be WR stars. The lines show the evolutionary model tracks, the blue lines represent the pre-WR evolution, the dashed black lines represent when $0.01 < X_{\rm surface} < 0.4$ and the solid black lines represent when $X_{\rm surface} < 0.01$. The left-hand panel shows the single-star models with masses 27, 30, 50, 80 and 120 $M_{\odot}$. The right-hand panel shows a few example binary models; the masses included are 10, 13, 15, 18, 20, 25, 30, 50, 80 and 120 $M_{\odot}$. In both panels, the red points are observed WR stars, with WN stars indicated by '*' and WC stars with '+'. The data are taken from Hamann et al. (2006) and Sander et al. (2012). The binary models cover a wider region in luminosity and temperature than the single-star models. The green contours indicate the region of the HR diagram covered by our Ibc progenitor populations.

must have $\log(L/{\rm L}_{\odot}) > 4.9$ to be a WR star. Stars with no surface hydrogen below this limit are still helium stars but are unlikely to be observed as WR stars. In summary, no stellar models of WR stars are perfect predictors of the observed WR star population but our models are at least close to reproducing the observational data here and in previous studies using BPASS.

We create the populations using the single-star and binary-star populations from BPASS. We predict the magnitudes by matching our stellar models to the Potsdam stellar atmosphere models of WR stars. We note that while we used these models above in Section 5.1, our method of using them here is separate. We match the stellar model radii and surface temperatures to the Potsdam WR models as described on the above website. For full details of the construction of the stellar evolution models, we refer the reader to Eldridge et al. (2008) and for the matching of models to stellar atmospheres to Eldridge & Stanway (2009).

We create four synthetic populations to compare to the progenitor non-detection limits. For both a single-star population and our fiducial binary- and single-star mix, we create two luminosity distributions with the following parameters.

(i) A WR star population with $X_{\rm surface} < 0.001$ and $\log(T_{\rm eff}/{\rm K}) > 4$. This is equivalent to the observed WR population.

(ii) A possible Ibc progenitor population with $X_{\rm surface} < 0.001$, $M > 2\,{\rm M}_{\odot}$ and we require the model to have completed core-helium burning. This restricts the population to models closer to core-collapse. This includes a range of radii for each model that is an approximate method to account for the uncertainty in the evolution of the progenitors. The population provides a range of possible magnitudes for the progenitors similar to the range allowed from various models of WR stars.

We have also created a third population based on the endpoints of our stellar models. We find however that the probabilities for these populations reproducing the non-detections are low and similar to the model WR populations with values of 4.6 and 1.5 per cent for single stars and binaries, respectively. The latter limit is low because of the *B*-band limit for SN 2002ap. This is because our models become cooler and therefore slightly brighter in the optical towards the end of their lives. However, as noted above this behaviour is different from that found by Ekström et al. (2012) and Yoon et al. (2012). In addition, the probabilities are sensitive to any extra dust absorption that has not have accounted for in calculating the *B*-band limit. We note that if we were to consider only *R*-band limits, which are more weakly affected by dust, the probabilities rise to 19 and 17 per cent, respectively. This difference is because using the endpoints along essentially describes only a line of points in the HR diagram rather than allowing for a range of values. One option would be to blur the stellar endpoints by considering different amount of intrinsic dust absorption or estimating what the radii of the WR stars would be if the envelope inflation did not occur. Attempting this would include arbitrary physical mechanisms that would allow us to achieve any fit we like. Therefore, we decided to use a similar method as we employed in Paper I: using population (ii) outlined above, and using the natural range of the temperatures and luminosities in the models themselves as they evolve towards the endpoint of their lives. Some vary little, such as the more massive WR stars, some vary more, especially the low-mass binary stars. Hence, our preferred quasi-progenitor population in an approximate method accounts for uncertainties in the WR models as well as other factors such as dust that might be produced in WR binaries (Crowther 2003).

Comparing the different luminosity distributions predicted from the various populations for different filters in Fig. 10, we see that

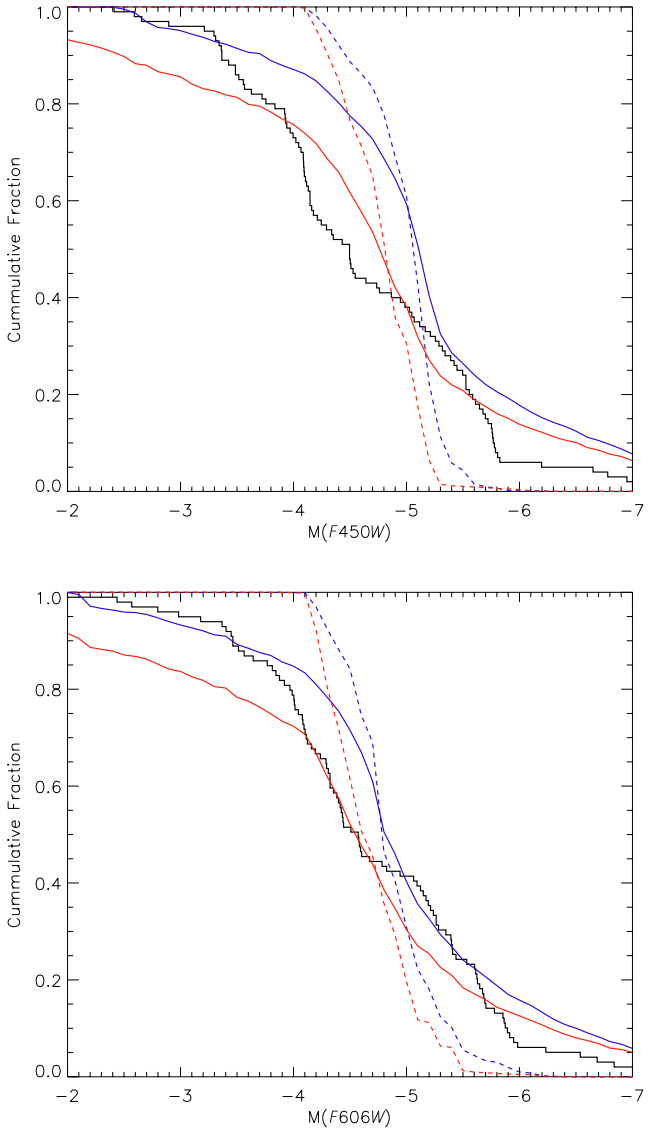

Figure 10. Cumulative frequency *F*450*W* (upper panel) and *F*606*W* (lower panel) magnitude distributions for observed WR stars (black line), single-star synthetic populations (dashed lines) and fiducial binary–single star mix (solid lines). The blue lines are for the synthetic WR population and the red lines the synthetic progenitor population.

for the *F*606*W* filter the observed and synthetic WR populations are similar. We note that the observed population here is the same as we use in Section 5.1 and not those in Fig. 9. The match for the *F*450*W* filter is slightly worse. We suggest that this is due to intrinsic dust extinction in the observed WR stars that is greater than that of the foreground extinction. We find a better match between the models and observations if we were to include on average $A_V = 0.5$ for the synthetic population but we do not apply it here. Furthermore, we see that our predicted progenitor magnitude range for the binary populations is greater than that for the single-star WR populations. This is because there is a wider range of helium and WR star masses allowed from binary evolution. Then the synthetic populations for the progenitor models are fainter than the synthetic WR populations. This is because the progenitor stars are hotter and less luminous than the general WR population. After core-helium burning, a WR star's luminosity is at the lowest point during its entire evolution.

The SN types resulting from the stars in these synthetic populations are determined using the parameters listed in Table 2. For the binary population, we include the contribution of the primary and secondary stars to the WR population. We also consider the companion flux when calculating the observed magnitude of the system. We see in Fig. 10 that the synthetic single-star WR population has a similar mean magnitude to the observed LMC WR population used above, but is not able to reproduce the spread of magnitudes. In contrast, the synthetic binary WR population is a much closer match to the observed distribution. This is because binary interactions increase the amount of mass-loss a star can undergo, and so widens the range of initial masses (and hence luminosities) which give rise to WR stars. In addition, the inclusion of the flux from the secondary in binary systems leads to some WR stars being apparently more luminous than possible from single stars alone.

We again stress that our method differs from that of Yoon et al. (2012), who only consider the very endpoint of each evolutionary track as the point of explosion. We use the predicted WR population and the population after core-helium burning. In using these, we are allowing for our synthetic progenitors to cover a region of the HR diagram rather than a narrow line of the endpoints. The advantage of this is that it gives us a range of possible magnitudes for each model, and hence allows us to take account of the uncertainties of stellar evolution and WR atmosphere modelling in our analysis in an approximate method rather than calculating numerous sets of binary models with varying input physics and mass-loss rates. Such a calculation would require 100 000s of stellar models and is beyond the scope of this paper. The method of Yoon et al. (2012), for example, is not incorrect in that they report the results of the endpoints of the calculations, but one has then to assume that these models are perfectly valid and describe accurately the unobserved processes in the last few thousand years before core-collapse. Hence, we suggest that our approach approximates modelling uncertainties, and we assume that we cannot definitively predict the endpoints. Especially considering we are attempting to model a population of non-detections.

We also note that our predicted magnitudes are different from those of Yoon et al. (2012). This is because that work is based on the narrow-band filter, v, rather than the broad-band filter, V, commonly available for progenitor detections. The narrow-band filter does not include emission line flux which can contribute significantly to the luminosity of WR stars, and v can be typically 0.5–1.0 mag fainter than broad-band *BVR*. This was also pointed out by Yoon et al. (2012), who convert between the two filters by assuming $V = v - 0.75$. In our method by calculating V directly, we account for the variation in how the two magnitudes are related depending on the effective temperature of the WR stars.

Using these synthetic populations we can again compare the progenitor limits to the various synthetic populations. From each SN, we can calculate a probability that the progenitor would remain undetected from the fraction of the synthetic population with a magnitude less than the limit. We then combine those individual probabilities to estimate the probability that no progenitor would have been observed in any of the pre-explosion images. We show the resulting probabilities and their combination in Table 6. As mentioned previously, the probability that we would not have detected a Type Ibc progenitor if the LMC WR sample is representative of the progenitors is 0.16. Similarly low values are found for all the progenitor models. The lowest values are for our WR populations and the progenitor population. The highest probabilities are for our single-star and binary populations from the end of core-helium burning to the end of the model, with 0.13 and 0.12, respectively.

All these low values are the result of the *B*-band limit for SN 2002ap. If we however account for the possibility of intrinsic dust around WR stars or switch the *R*-band limit which is less affected by extinction, these probabilities would increase. We note that for the binary populations, the probability of detecting SN 2002ap is nearly double that for the single-star populations. The reason why there is little difference between the overall probabilities is that the binary stars also predict more luminous progenitors than the single-star population. This perhaps gives the false impression that single stars are more likely to be the possible progenitors. If we consider only the deepest limits SNe 2002ap, 2004gn and 2010br, then the binary population again is slightly more favoured.

In conclusion, while we favour a mixed population of WR stars and lower mass helium stars in binaries as the progenitors of Type Ibc SNe, we cannot set strong constraints from the current limits and non-detections. We are also limited by our limited understanding of WR star evolution and which stellar models correctly reproduce the observed population of WR stars and progenitors of Type Ibc SNe.

One thing that is apparent is that the low probabilities we obtain indicate that the Ibc progenitor population is fainter than expected from the magnitudes of WR stars. Therefore, other factors could be at play making it more difficult to observe Ibc progenitors. For example, either dust being produced to decrease their luminosity (e.g. Crowther 2003) or that the predictions of Yoon et al. (2012) and Ekström et al. (2012) are correct and the progenitors should be hotter at the time of core-collapse than we predict.

6 DISCUSSION

There are two main candidates for the progenitors of Type Ibc SNe: WR stars ($M \gtrsim 20\,\mathrm{M}_{\odot}$) and lower mass helium stars. The former will experience mass-loss which is primarily due to stellar winds and will effectively evolve as single stars. The latter are the result of close binary evolution, where the mass-loss is due to binary interactions of Roche lobe overflow or common-envelope evolution. Both progenitor channels are plausible. WR stars are commonly observed in star-forming environments, but to the best of our knowledge no completely hydrogen-free low-mass helium stars are known (with a core mass that will create an O–Ne–Mg or Fe core and experience core-collapse) and their existence remains conjecture.

6.1 Arguments in favour of interacting binaries as progenitors of Ibc SNe

From the limits presented in Section 5, it is difficult to distinguish between the different progenitor populations. However considering the deepest limit alone, SN 2002ap is more likely to have been detected if WR stars were the sole progenitors of Type Ibc SNe. This one progenitor was less likely to have been observed if it were a binary system as stated by Crockett et al. (2007). The number of non-detections to date suggest that we do not fully understand the evolution of hydrogen-free stars. We do suggest however because of the lower magnitudes of WR stars as they approach core-collapse as also discussed by other authors that at the moment the number of non-detections are not enough to constrain the population directly.

The uncertainties in the models which make a comparison difficult include how the stars evolve after core-carbon burning, and how much dust might a low-mass helium star create in a binary. Systems such as those discussed by Crowther (2003) would be difficult to observe, and alter our predicted luminosity distributions significantly. Therefore, from the progenitor detections, we can conclude that there is only very weak evidence from the deepest non-detections that binaries are the more favoured progenitors.

The strongest case for binary stars contributing to the Type Ib/c SN progenitor populations can be made by the fact we can reproduce the observed relative rate of different SN types (Podsiadlowski et al. 1992; De Donder & Vanbeveren 1998; Yoon et al. 2010). Current single-star models predict too many Type II SNe; however, recent studies have indicated that the mass-loss rates of RSGs remain a large source of uncertainty (Yoon & Cantiello 2010; Georgy 2012).

Currently no single-star model can fit the population of RSGs, WR stars and SN rates simultaneously. The Geneva rotating stellar evolution models have come very close (Ekström et al. 2012), but assume a single initial rotational velocity rather than a distribution of rotation velocities as are observed (Hunter et al. 2008). In contrast, binary models can also come close to reproducing both observed stellar populations and relative SN rates with a reasonable distribution of initial binary parameters (e.g. Vanbeveren et al. 1998; Belkus et al. 2003; Eldridge et al. 2008; Eldridge & Stanway 2009). Also they are able to match individual binary systems that have been observed (e.g Eldridge 2009). In our binary population model which fits best both the observed relative SN rates and the non-detection of a Type Ibc progenitor, we find that single WR stars contribute one-fifth of Ibc SNe, with binary systems giving rise to the rest. Furthermore, in our synthetic population only half of the SNe will be in a binary at the time of core-collapse, the remainder being apparently single. This is because binaries are either unbound in the first SN or have a compact companion at the time of the second SN. Deep post-explosion images with the *HST* at the sites of Type Ibc SNe may help identify the surviving binary companion of the progenitor as described by Kochanek (2009).

It is important to note that our binary population model also predicts the location on the HR diagram of the progenitors of hydrogen-poor Type IIb and IIL SNe. In Fig. 12, we show a cartoon HR diagram based on our synthetic population, where the YSG progenitors lie above our predicted location for the hydrogen-deficient SNe. We note that this matches the observed progenitors of SNe 1993J, 2008ax, 2009kr and 2011dh, which are intermediate between the Type Ibc progenitors and hydrogen-rich IIP RSG progenitors.

Hence, the question then is, where are the binary systems that harbour Ibc progenitor systems? If we examine our binary evolution models more closely, we find that stars below approximately $15\,\mathrm{M}_{\odot}$ spend only a very small fraction of their total lifetime without hydrogen in their structure before core-collapse. This is shown in Fig. 11, which displays the hydrogen mass fraction of single-star and binary models before the end of the stellar models. Stars less massive than $15\,\mathrm{M}_{\odot}$ retain a low-mass hydrogen envelope that is helium rich. This is only lost a short time before core-collapse. In the right-hand panel of Fig. 12, the envelope is lost as the stars evolve from their hottest extent to cooler effective temperatures. Stars with parameters similar to these stars have been observed and are objects such as V Sagittae, WR7a and HD 45166[17] (Steiner & Diaz 1998; Oliveira et al. 2003; Steiner & Oliveira 2005; Groh et al. 2008). The objects are often discarded as potential Ibc progenitors due to the presence of hydrogen on their surface. In Fig. 11, however, we show the surface hydrogen mass fraction for our models which indicate that these possible Type Ibc progenitors are hiding large helium

[17] HD 45166 is slightly more hydrogen rich than predicted by our models. This is probably a result of the secondary star filling its Roche lobe at periastron and transferring hydrogen back on to the primary (Steiner & Oliveira 2005).

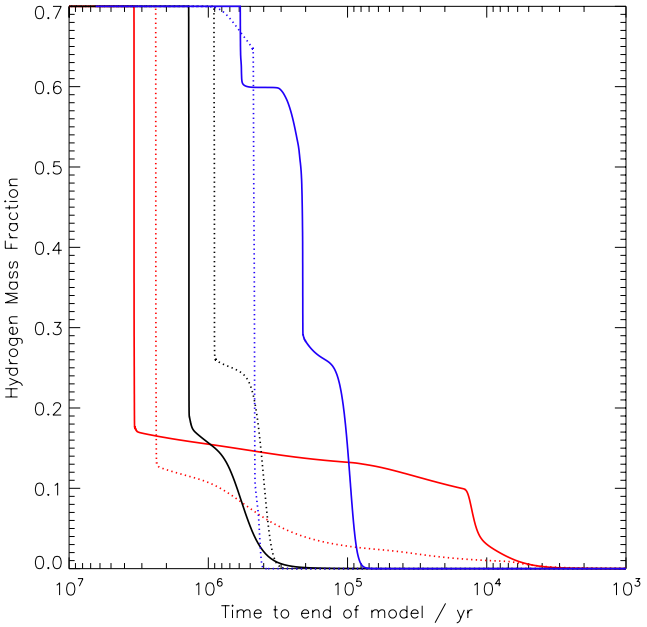

Figure 11. Diagram of the hydrogen mass fraction of different progenitor models before the end of our models. The solid and dotted blue lines are for 30 and 50 $M_\odot$ single-star models, respectively. The solid and dotted black lines are for 15 and 20 $M_\odot$ binary models, respectively. The solid and dotted red lines are for 10 and 12 $M_\odot$ binary models, respectively.

cores and the residual hydrogen could be stripped in the last 10^4 yr of their life; hence, it may not be surprising that they exist within this configuration and that completely hydrogen-free He stars in binaries are difficult to locate. This may seem unexpected but we stress that a binary interaction does not immediately lead to complete loss of the hydrogen envelope in a star. Roche lobe overflow or common-envelope evolution removes most of the hydrogen envelope but eventually an envelope mass is reached at which point it collapses back within the star's Roche lobe. Stellar winds are then responsible for removing the remaining gas. For stars above 15 $M_\odot$, the winds are strong enough to do this during helium burning. Below this limit it is not until the star evolves to a helium giant that the mass-loss rate becomes strong enough to drive off the hydrogen before core-collapse. We note that at lower metallicity weaker winds may reduce the number of Type Ibc SNe from these binary stars; therefore, the Type Ibc rate will decrease at lower metallicities.

The other piece of observational evidence that supports helium stars as SN progenitors is the ejecta masses determined from the studies of the light curves and observed ejecta velocities. There are now many Ibc SNe with well-sampled light curves, and some with data stretching through the nebular phase. Simple analytical models following Arnett (1982) can estimate ejecta mass and ^{56}Ni mass from the rise time, width and peak of the light curve. More sophisticated radiative transfer modelling with Monte Carlo techniques (for example, Nakamura et al. 2001; Mazzali et al. 2007; Dessart et al. 2011) has been used to determine also the kinetic energy from the velocity information in the spectra. A summary of the main results for Type Ibc SNe is compiled in Table 7. The models of the most common Ibc SNe types in the local Universe (within our 28 Mpc volume), and those for which we have constrained the properties of the progenitors, tend to be between 1 and 3 $M_\odot$. This fact has recently been highlighted by sophisticated modelling of Ibc SNe by Hachinger et al. (2012) and Dessart et al. (2012). In addition, Drout et al. (2011) presented a homogeneous study of the ejecta masses of 25 Ibc SNe and found similarly low masses consistently through the sample. There are a small percentage of the overall Ic SNe class that have very broad light curves and usually, but not always, high ejecta velocities (often called Ic-BL, or broad-lined Ic). There is some evidence that they have significantly higher ejecta masses. Their light curves are significantly broader and a higher ejecta mass

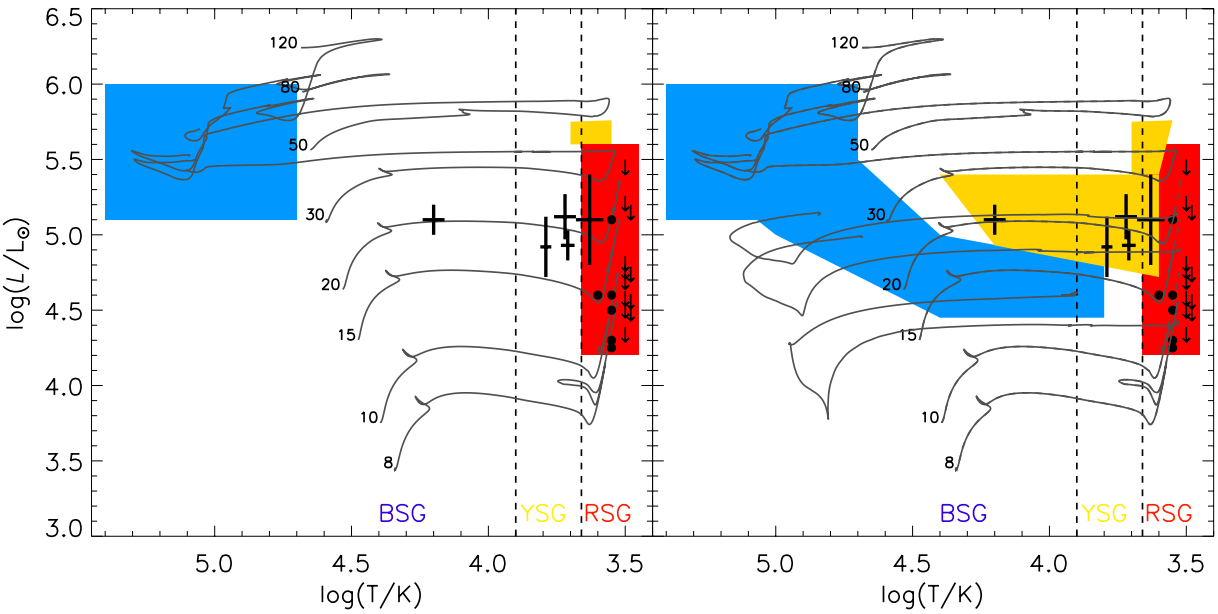

Figure 12. Cartoon HR diagrams of SN progenitors; the red, yellow and blue regions show the expected location of progenitors for Type IIP, other Type II and Type Ib/c SNe. The left-hand panel shows the single-star scenario. The solid lines show the evolution tracks for stars with masses given at their initial location. The right-hand panel shows the binary scenario with the solid tracks at 10, 15 and 20 $M_\odot$ showing binary evolution tracks and the dashed lines the single-star tracks. In both plots, the points with error bars show the locations of SNe 1987A, 1993J, 2008cn, 2009kr and 2011dh (Podsiadlowski 1992; Maund et al. 2004, 2011; Elias-Rosa et al. 2009, 2010; Fraser et al. 2010), respectively. The circles show the progenitor locations of observed Type IIP progenitors and the arrows the upper limits for these progenitors (Smartt et al. 2009).

Table 7. Measured ejecta masses for Ibc SNe from the literature. These are light-curve modelling. In some cases, an estimated mass of oxygen is also determined from spectral modelling and is added here for reference. Typical stellar evolution models predict that a 25 $M_\odot$ star would produce between 2 and 4 $M_\odot$ of oxygen during its nucleosynthetic evolution.

SN	Type	O mass/ $M_\odot$	Total ejecta mass/ $M_\odot$	Refs
2007Y	Ib	0.2	0.4	Stritzinger et al. (2009)
1994I	Ic	–	0.7	Valenti et al. (2008a)
2007gr	Ic	0.8	1–2	Mazzali et al. (2010), Hunter et al. (2009)
2006aj	Ic	1.3	2	Mazzali et al. (2006), Maeda et al. (2007)
2002ap	Ic	1.2	2.5	Mazzali et al. (2007)
2003jd	Ic	–	3	Valenti et al. (2008a)
2008D	Ib	1.1	3.6	Dessart et al. (2012)
2004aw	Ic	–	5	Valenti et al. (2008a)
2009jf	Ib	–	5–7	Valenti et al. (2011)
1997ef	Ic	–	7–10	Mazzali, Iwamoto & Nomoto (2000)
1998bw	Ic	2–3	10	Nakamura et al. (2001)
2011bm	Ic	5–10	7–17	Valenti et al. (2012)
Sample average	Ib	–	$2^{+1.1}_{-0.8}$	Drout et al. (2011)
Sample average	Ic	–	$1.7^{+1.4}_{-0.9}$	Drout et al. (2011)
Sample average	Ic-BL	–	$4.7^{+2.3}_{-1.8}$	Drout et al. (2011)

is the obvious way to explain the differences with a similar physical model. However, these Ic-BL are rare, with only one (SN 2002ap) having been discovered within 28 Mpc in the duration of our survey. Their contribution to the overall Ibc SN population is likely less than 3 per cent (see Section 2) and these could conceivably be from higher mass He or CO stars. WR stars would be the obvious candidates for some of these Type Ic SNe (Dessart et al. 2012).

In Table 7 we also list the oxygen ejecta mass where it has been estimated by model application. Generally, this is around 1 $M_\odot$ or lower, also supporting the idea that the bulk of the Ibc SNe are not from WR star progenitors with ZAMS masses $\geq$25 $M_\odot$ (see Mazzali et al. 2010).

We predict ejecta masses from the synthetic populations as described in Eldridge & Tout (2004). These should be considered upper limits as we do not evolve our models to Fe-core formation and so may underestimate the final remnant mass. Our binary progenitor models (which mainly form neutron-star remnants) have an average ejecta mass of $4.2 \pm 2.4\,M_\odot$ while single-star progenitors (which mainly form black hole remnants) have ejecta masses in the range $6.6 \pm 0.9\,M_\odot$. This further supports the idea that *normal* Type Ibc SNe come from helium stars formed in binaries with initial masses below 20 $M_\odot$ and form neutron stars at core-collapse.

6.2 Arguments in favour of WR stars as progenitors of Ibc SNe

Recently, much work has been done on the stellar populations near the location of SNe (e.g. Leloudas et al. 2011; Murphy et al. 2011; Anderson et al. 2012). These range from studying the resolved stellar populations using high-resolution *HST* data, such as that presented here (Murphy et al. 2011), to lower resolution ground-based data that typically use Hα to probe regions of star formation. Using the latter technique, Anderson et al. (2012) propose that Type Ibc SNe tend to show stronger spatial association with Hα emission in galaxies compared to Type II SNe, and Type IIP in particular. As Hα emission originates in young clusters and associations, their interpretation is that Type Ibc SNe may arise from significantly higher mass stars than Type IIP. They also find that the spatial correlation is strongest for Type Ic SNe, even more so than Type Ib. Anderson et al. (2012) interpret this as an increasing mass sequence, with Type II SNe coming from the lowest mass stars and Ib and Ic from progressively higher mass. This would argue in favour of Ibc progenitors being significantly higher mass stars than progenitors of IIP SNe, and since we know that IIP SNe arise in 8–17 $M_\odot$ stars (Smartt 2009; Smartt et al. 2009) then this might suggest WR progenitors of Type Ibc SNe with initial mass $\geq$20 $M_\odot$.

These SNe are typically at distances of 50–100 Mpc and the ground-based imaging does not specifically identify the host H II region, a fact which led Crowther (2013) to study the environments of the closest 39 CCSNe in nearby ($\leq$15 Mpc) and low-inclination galaxies. While Ibc SNe are nearly twice as likely to be associated with nearby H II emission, Crowther (2013) finds that these nebulae are long-lived, giant H II regions with typical lifetimes more than 20 Myr. Hence, the association only provides weak constraints on Ibc progenitor masses. Binary evolution would extend the period during which Type Ibc SNe occur up to 20 Myr, and this is still roughly in agreement with observed population ages from the H II region analysis. The greater mean age of binary SN progenitors is also in accord with the absence of any H II regions or large young stellar populations at the site of the Type Ibc SNe in our sample. The typical lifetime of an H II region is between 3 and 5 Myr, i.e. shorter than the lifetime of most binary Type Ibc progenitors. Only the most massive regions such as NGC 604 or 30 Doradus have more extended periods of star formation, and such systems are rare.

There are two other factors that may have prevented us from detecting WR progenitor stars. First, it is possible that WR stars evolve rapidly in the later stages of their lives. This could mean that, just prior to core-collapse, they appear significantly different from the WR stars we observe in the LMC, possibly getting hotter and fainter in the last 5 per cent of their lifetimes. This has been investigated by Yoon et al. (2012), and Ekström et al. (2012) indicate similar evolution. However, we suggest that progenitors are slightly more observable than this. One reason for the difference is due to Yoon et al. (2012) using mainly magnitudes in the narrow band M_v with a constant correction factor to M_V rather than allowing for the range of differences between the magnitudes of 0.5 and 1.0. Also their models end their lives with higher surface temperatures than we find which again makes the model progenitors dimmer at optical magnitudes. Secondly, we may have underestimated the extinctions

towards the WR star progenitors (and hence our detection limits are not as deep as we have presented here), or WR stars could create and eject dust in the last fraction of their lifetimes. The values for $E(B-V)$ used in Table 4 are those estimated for the foreground line of sight (including host galaxy extinction where possible). The distribution is characterized by a mean and standard deviation of $\langle E(B-V)\rangle = 0.22 \pm 0.28$, which is similar to the extinctions estimated by Bibby & Crowther (2010, 2012) towards WR stars in NGC 5068 and NGC 7793. In addition, we have added our estimates of extinction to the limiting magnitudes, whereas for the LMC sample we have simply taken foreground Milky Way extinction. Any extra internal LMC or circumstellar extinction would tend to make the LMC reference sample brighter for our comparison purposes and the restrictions tighter. In this study, we have no ability to disentangle the foreground extinction from circumstellar; hence, we have not employed the new and physically consistent methods of Kochanek, Khan & Dai (2012). If a Ibc progenitor were found, then it would be necessary to consider the circumstellar extinction separately to foreground ISM as discussed by Kochanek et al. (2012) as is the case for SN2012aw.

7 CONCLUSIONS

We have used the observed limits on the progenitors of Type Ibc SNe in pre-explosion images, the observed relative rates for different SN types and a binary population model to study their progenitor population. From both sets of data, we find that it is difficult to constrain the progenitor population. However, for the SN with the deepest limits, SN 2002ap, a single stellar population is disfavoured. Because of this and attempting to match the observed relative SN rates, we suggest that the bulk of the Type Ibc SNe most likely arise from low-mass progenitors which have been stripped by a binary companion. This scenario is also supported by the fact that the ejecta masses from Ibc SNe are, in general, too low to be from massive WR stars.

The favoured progenitors are therefore the hypothetical low-mass helium stars. However, no such hydrogen-free stars with masses large enough to experience core-collapse are known in the Galaxy. Our stellar models of these systems indicate that this is actually to be expected. The binary interaction that seals these stars to their final fate does not remove all hydrogen from the stellar surface and leaves approximately a few times $0.1\,M_{\odot}$. This is removed by stellar winds as the star evolves at the end of core-helium burning. These objects would appear similar to observed binary systems such as V Sagittae, WR7a and HD 45166. Therefore, we suggest that the final fate of these systems will be Type Ibc SNe. Further detailed study and modelling of these systems are required to confirm this.

While there are some Ic SNe which have broad light curves and likely large ejecta masses, they are much rarer by volume compared to the bulk of the normal Ibc SN population. It is still possible that these Ic SNe do come from massive WR stars; however, Podsiadlowski et al. (2004) show that even if one assumes that only stars above $80\,M_{\odot}$ produce broad-lined and broad-light-curve Ic SNe, then the observed rate of such SNe is still too low. Hence, the massive, classical WR population does not produce the majority of the normal Ibc SNe we see within 28 Mpc. However, they could contribute to this population or supply progenitor systems producing rarer Type Ibc events. It is possible that some fraction of WR stars form black holes in such a way that they produce faint SNe or no visible display.

ACKNOWLEDGEMENTS

The research leading to these results has received funding from the European Research Council under the European Union's Seventh Framework Programme (FP7/2007-2013)/ERC Grant agreement no. [291222] (PI: Smartt). The research of JRM is supported through a Royal Society University Research Fellowship. We thank Erkki Kankare for information on SN 2005at. We also thank Nancy Elias-Rosa and Max Strizinger for sharing the spectra of 2011br and 2011am. We thank Brad Cenko for information on SN 2004gn. We also thank Stefano Benetti and Nancy Elias Rosa for access to an NTT image of SN2011am and a spectrum of SN2011hp from the ESO Large Programme 184.D-1140 'Supernova Variety and Nucleosynthesis Yields'. We thank Andreas Sander for clarifying some details of the Potsdam WR atmosphere models. We also thank the anonymous referee, Dirk Lennarz, Lev Yungelson, Christopher Kochanek, Danny Van Beveren, Alexander Tutukov, Luca Izzo and Jorge Rueda for constructive comments that improved this paper.

REFERENCES

Aldering G., Humphreys R. M., Richmond M., 1994, AJ, 107, 662
Anderson J. P., Habergham S. M., James P. A., Hamuy M., 2012, MNRAS, 424, 1372
Arcavi I. et al., 2011, ApJ, 742, 18
Arnett W. D., 1982, ApJ, 253, 785
Begelman M. C., Sarazin C. L., 1986, ApJ, 302, L59
Belczynski K., Kalogera V., Bulik T., 2002, ApJ, 572, 407B
Belkus H., Van Bever J., Vanbeveren D., van Rensbergen W., 2003, A&A, 400, 429
Berger E., 2010, Astron. Telegram, 2655
Bibby J. L., Crowther P. A., 2010, MNRAS, 405, 2737
Bibby J. L., Crowther P. A., 2012, MNRAS, 420, 3091
Bock G., Parker S., Brimacombe J., 2011, CBET, 2667, 1
Botticella M. T. et al., 2009, MNRAS, 398, 1041
Botticella M. T., Smartt S. J., Kennicutt R. C., Cappellaro E., Sereno M., Lee J. C., 2012, A&A, 537, A132
Branch D. et al., 2002, ApJ, 566, 100
Breysacher J., Azzopardi M., Testor G., 1999, A&AS, 137, 117
Brunthaler A., Menten K. M., Reid M. J., Henkel C., Bower G. C., Falcke H., 2009, A&A, 499, L17
Brunthaler A. et al., 2010, A&A, 516, 27
Burrows A., 2013, Rev. Mod. Phys., 85, 245
Chevalier R. A., Soderberg A. M., 2010, ApJ, 711, L40
Chornock R., Filippenko A. V., 2001, IAU Circ., 7577, 2
Chornock R., Filippenko A. V., Li W., Foley R. J., Reitzel D., Rich R. M., 2007, CBET, 1036, 1
Crockett R. M. et al., 2007, MNRAS, 381, 835
Crockett R. M. et al., 2008, ApJ, 672, L99
Crockett R. M., Smartt S. J., Pastorello A., Eldridge J. J., Stephens A. W., Maund J. R., Mattila S., 2011, MNRAS, 410, 2767
Crowther P. A., 2003, Ap&SS, 285, 677
Crowther P. A., 2007, ARA&A, 45, 177
Crowther P. A., 2013, MNRAS, 428, 1927
De Donder E., Vanbeveren D., 1998, A&A, 333, 557
Dennefeld M., Patris J., 2000, IAU Circ., 7532, 3
Dessart L., Hillier D. J., Livne E., Yoon S.-C., Woosley S., Waldman R., Langer N., 2011, MNRAS, 414, 2985
Dessart L., Hillier D. J., Li C., Woosley S., 2012, MNRAS, 424, 2139
Drout M. R. et al., 2011, ApJ, 741, 97
Ekström S. et al., 2012, A&A, 537, A146
Eldridge J. J., 2009, MNRAS, 400, L20
Eldridge J. J., Tout C. A., 2004, MNRAS, 353, 87
Eldridge J. J., Stanway E. R., 2009, MNRAS, 400, 1019
Eldridge J. J., Stanway E. R., 2012, MNRAS, 419, 479
Eldridge J. J., Izzard R. G., Tout C. A., 2008, MNRAS, 384, 1109

Eldridge J. J., Langer N., Tout C. A., 2011, MNRAS, 411, 3501
Elias-Rosa N. et al., 2009, ApJ, 706, 1174
Elias-Rosa N. et al., 2010, ApJ, 714, L254
Elmhamdi A., Tsvetkov D., Danziger I. J., Kordi A., 2011, ApJ, 731, 129
Fassia A. et al., 2001, MNRAS, 325, 907
Filippenko A. V., 1997, ARA&A, 35, 309
Filippenko A. V., De Breuck C., 1998, IAU Circ., 6994, 3
Filippenko A. V., Chornock R., 2001, IAU Circ., 7638, 1
Filippenko A. V., Chornock R., 2003, IAU Circ., 8211, 2
Filippenko A. V., Foley R. J., Modjaz M., 2000, IAU Circ., 7547, 2
Foley R. J., Smith N., Ganeshalingam M., Li W., Chornock R., Filippenko A. V., 2007, ApJ, 657, 105
Foley R. J. et al., 2009, AJ, 138, 376
Foley R. J. et al., 2010a, AJ, 140, 1321
Foley R. J., Brown P. J., Rest A., Challis P. J., Kirshner R. P., Wood-Vasey W. M., 2010b, ApJ, 708, 61
Foley R. J., Berger E., Fox O., Levesque E. M., Challis P. J., Ivans I. I., Rhoads J. E., Soderberg A. M., 2011, ApJ, 732, 32
Fraser M., Smartt S. J., Crockett M., Mattila S., Stephens A. G.-Y. A., Roth K., 2009, Astron. Telegram, 2131
Fraser M. et al., 2010, ApJ, 714, L280
Fraser M., Maund J. R., Smartt S. J., Bufano F., Benetti S., Elias-Rosa N., 2011, Astron. Telegram, 3371
Fraser M. et al., 2013, MNRAS, 433, 1312
Gal-Yam A., Ofek E. O., Shemmer O., 2002, MNRAS, 332, 73
Gal-Yam A. et al., 2005, ApJ, 630, 29
Gaskell C. M., Cappellaro E., Dinerstein H. L., Garnett D. R., Harkness R. P., Wheeler J. C., 1986, ApJ, 306, L77
Georgy C., 2012, A&A, 538, L8
Gerardy C. L., Fesen R. A., Nomoto K., Maeda K., Hoflich P., Wheeler J. C., 2002, PASJ, 54, 905
Gräfener G., Owocki S. P., Vink J. S. G., 2012, A&A, 538, A40
Graham J., Li W., 2003, IAU Circ., 8207, 1
Groh J. H., Oliveira A. S., Steiner J. E., 2008, A&A, 485, 245
Hachinger S., Mazzali P. A., Taubenberger S., Hillebrandt W., Nomoto K., Sauer D. N., 2012, MNRAS, 422, 70
Hamann W.-R., Gräfener G., 2004, A&A, 427, 697
Hamann W.-R., Gräfener G., Liermann A., 2006, A&A, 457, 1015
Heger A., Fryer C. L., Woosley S. E., Langer N., Hartmann D. H., 2003, ApJ, 591, 288
Hendry M. A. et al., 2005, MNRAS, 359, 906
Hess K. M., Pisano D. J., Wilcots E. M., Chengalur J. N., 2009, ApJ, 699, 76
Hillebrandt W., Niemeyer J. C., 2000, ARA&A, 38, 191
Hoffman D. et al., 2011, Astron. Telegram, 3160
Horiuchi S., Beacom J. F., Kochanek C. S., Prieto J. L., Stanek K. Z., Thompson T. A., 2011, ApJ, 738, 154
Hunter I., Lennon D. J., Dufton P. L., Trundle C., Simn-Daz S., Smartt S. J., Ryans R. S. I., Evans C. J., 2008, A&A, 479, 541
Hunter D. J. et al., 2009, A&A, 508, 371
Iben I., Jr, Tutukov A. V., 1985, ApJS, 58, 661
Ishii M., Ueno M., Kato M., 1999, PASJ, 51, 417I
Iwamoto K., Nomoto K., Hoflich P., Yamaoka H., Kumagai S., Shigeyama T., 1994, ApJ, 437, L115
Janka H.-T., 2012, Annu. Rev. Nucl. Part. Sci., 62, 407
Jha S., Riess A. G., Kirshner R. P., 2007, ApJ, 659, 122
Kawabata K. S. et al., 2002, ApJ, 580, 39
Kinugasa K., Kawakita H., Yamaoka H., 2004, IAU Circ., 8456, 2
Kochanek C. S., 2009, ApJ, 707, 1578
Kochanek C. S., Khan R., Dai X., 2012, ApJ, 759, 20
Langer N., 2012, ARA&A, 50, L107
Leloudas G. et al., 2011, A&A, 530, A95
Lennarz D., Altmann D., Wiebusch C., 2012, A&A, 538, 120
Levesque E. M., Stringfellow G. S., Ginsburg A. G., Bally J., Keeney B. A., 2012, preprint (arXiv:1211.4577)
Li W. D., Modjaz M., Treffers R. R., Filippenko A. V., Leonard D. C., 1998, IAU Circ., 6882, 1
Li W. D. et al., 2003, PASP, 115, 453
Li W., Yamaoka H., Itagaki K., 2004, CBET, 100, 1
Li W. et al., 2011, MNRAS, 412, 1441
Madison D., Li W., 2007, CBET, 1034, 1
Maeda K., 2013, ApJ, 762, 14
Maeda K. et al., 2007, ApJ, 658, L5
Marchili N. et al., 2010, A&A, 507, 47
Margutti R. et al., 2013, preprint (arXiv:1306.0038)
Massey P., 2002, ApJS, 141, 81
Massey P., 2003, ARA&A, 41, 15
Matheson T., Jha S., Challis P., Kirshner R., Calkinas M., 2001, IAU Circ., 7563, 2
Mattila S., Greimel R., Gerardy C., Meikle W. P. S., 2005, IAU Circ., 8474, 1
Mattila S. et al., 2012, ApJ, 756, 111
Mattila S., Fraser M., Smartt S. J., Meikle W. P. S., Romero-Canizales C., Crockett R. M., Stephens A., 2013, MNRAS, 431, 2050
Mauerhan J. C. et al., 2013, MNRAS, 430, 1801
Maund J. R., Smartt S. J., 2005, MNRAS, 360, 288
Maund J. R., Smartt S. J., Kudritzki R. P., Podsiadlowski P., Gilmore G. F., 2004, Nat, 427, 129
Maund J. R., Smartt S. J., Schweizer F., 2005, ApJ, 630, L33
Maund J. R. et al., 2011, ApJ, 739, 37
Maxwell A. J., Graham M. L., Parker A., Sadavoy S., Pritchet C. J., Hsiao E. Y., Balam D. D., 2010, CBET, 2245, 2
Mazzali P. A., Iwamoto K., Nomoto K., 2000, ApJ, 545, 407
Mazzali P. A. et al., 2002, ApJ, 572, 61
Mazzali P. A. et al., 2006, Nat, 442, 1018
Mazzali P. A. et al., 2007, ApJ, 670, 592
Mazzali P. A., Maurer I., Valenti S., Kotak R., Hunter D., 2010, MNRAS, 408, 87
Meikle P., Lucy L., Smartt S. J., Leibundgut B., Lundqvist P., Ostensen R., 2002, IAU Circ., 7811, 2
Monard L. A. G., 2004, IAU Circ., 8454, 1
Monard L. A. G., Stritzinger M., Foley R. J., 2011, CBET, 2899, 1
Moriya T., Tominaga N., Tanaka M., Nomoto K., Sauer D. N., Mazzali P. A., Maeda K., Suzuki T., 2010, ApJ, 719, 1445
Morrell N., Stritzinger M., Ho L., 2011, CBET, 2667, 2
Murphy J. W., Jennings Z. G., Williams B., Dalcanton J. J., Dolphin A. E., 2011, ApJ, 742, L4
Nakamura T., Mazzali P. A., Nomoto K., Iwamoto K., 2001, ApJ, 550, 991
Nakano S, Hirose Y., Kushida R., Kushida Y., Li W., 2002, IAU Circ., 7810, 1
Narayan G. et al., 2011, ApJ, 731, L11
Nevski V., Maksym A., Elenin L., Schwartz M., 2010, CBET, 2245
Nomoto K. I., Iwamoto K., Suzuki T., 1995, Phys. Rep., 256, 173
Oliveira A. S., Steiner J. E., Cieslinski D., 2003, MNRAS, 346, 963
Paczyński B., 1967, Acta Astron., 17, 355
Paragi Z. et al., 2010, Nat, 463, 516
Pastorello A. et al., 2005, MNRAS, 360, 950
Pastorello A. et al., 2007, Nat, 447, 829
Pastorello A. et al., 2013, ApJ, 767, 1
Podsiadlowski P., 1992, PASP, 104, 717
Podsiadlowski Ph, Joss P. C., Hsu J. J. L., 1992, ApJ, 391, 246
Podsiadlowski P., Mazzali P. A., Nomoto K., Lazzati D., Cappellaro E., 2004, ApJ, 607, L17
Poznanski D., Ganeshalingam M., Silverman J. M., Filippenko A. V., 2011, MNRAS, 415, L81
Poznanski D., Prochaska J. X., Bloom J. S., 2012, MNRAS, 426, 1465
Prieto J. L., Brimacombe J., Drake A. J., Howerton S., 2013, ApJ, 763, 27
Puckett T., Langoussis A., Garradd G. J., 2000, IAU Circ., 7530, 1
Quimby R., Gerardy C., Hoeflich P., Wheeler J. C., Shetrone M., Riley V., 2004, IAU Circ., 8446, 1
Saha A., Thim F., Tammann G. A., Reindl B., Sandage A., 2006, ApJS, 165, 108
Sana H. et al., 2012, Sci, 337, 444
Sander A., Hamann W.-R., Todt H., 2012, A&A, 540, 144
Saviane I., Hibbard J. E., Rich R. M., 2004, AJ, 127, 660

Saviane I., Momany Y., da Costa G. S., Rich R. M., Hibbard J. E., 2008, ApJ, 678, 179
Schlegel D. J., Finkbeiner D. P., Davis M., 1998, ApJ, 500, 525
Schweizer F. et al., 2008, ApJ, 136, 1482
Silverman J. M., Cenko S. B., Miller A. A., Nugent P. E., Filippenko A. V., 2012, CBET, 3052, 2
Smartt S. J., 2009, ARA&A, 47, 63
Smartt S. J., Vreeswijk P. M., Ramirez-Ruiz E., Gilmore G. F., Meikle W. P. S., Ferguson A. M. N., Knapen J. H., 2002, ApJ, 572, 147
Smartt S. J., Maund J. R., Gilmore G. F., Tout C. A., Kilkenny D., Benetti S., 2003, MNRAS, 343, 735
Smartt S. J., Eldridge J. J., Crockett R. M., Maund J. R., 2009, MNRAS, 395, 1409
Smith N. et al., 2009, ApJ, 697, 49
Smith N. et al., 2010, AJ, 139, 1451
Smith N., Li W., Filippenko A. V., Chornock R., 2011a, MNRAS, 412, 1522S
Smith N., Li W., Silverman J. M., Ganeshalingam M., Filippenko A. V., 2011b, MNRAS, 415, 773
Soderberg A. M., Brunthaler A., Nakara E., Chevalier R. A., Bietenholz M. F., 2010, ApJ, 725, 922
Steiner J. E., Diaz M. P., 1998, PASP, 110, 276S
Steiner J. E., Oliveira A. S., 2005, A&A, 444, 895
Stritzinger M. et al., 2009, ApJ, 696, 713
Swift B., Li W. D., Filippenko A. V., 2001, IAU Circ., 7618, 1
Takada-Hidai M., Aoki W., Zhao G., 2002, PASJ, 54, 899
Tanaka M., Kawabata K. S., Maeda K., Hattori T., Nomoto K., 2008, ApJ, 689, 1191
Tarchi A., Neininger N., Greve A., Klein U., Garrington S. T., Muxlow T. W. B., Pedlar A., Glendenning B. E., 2000, A&A, 358, 95
Taubenberger S., Pastorello A., Benetti S., Aceituno J., 2005, IAU Circ., 8474, 3
Tsvetkov D. Y., 2006, Perem. Zvezdy, 26, 3
Tully R. B., Rizzi L., Shaya E. J., Courtois H. M., Makarov D. I., Jacobs B. A., 2009, AJ, 138, 323
Turatto M., Benetti S., Cappellaro E., 2003, in Hillebrandt W., Leibundgut B., eds, From Twilight to Highlight: The Physics of Supernovae. Springer-Verlag, Berlin, p. 200
Turatto M., Benetti S., Pastorello A., 2007, in Immler S., Weiler K., McCray R., eds, AIP Conf. Ser. Vol. 937, Supernova 1987A: 20 Years After: Supernovae and Gamma-Ray Bursters. Am. Inst. Phys., New York, p. 187
Tutukov A. V., Yungelson L. R., Iben I., Jr, 1992, ApJ, 386, 197
Ugliano M., Janka H.-T., Marek A., Arcones A., 2012, ApJ, 757, 69
Valenti S. et al., 2008a, MNRAS, 383, 1485
Valenti S. et al., 2008b, ApJ, 673, 155
Valenti S. et al., 2009, Nat, 459, 674
Valenti S. et al., 2011, MNRAS, 416, 3138
Van Dyk S. D., Li W., Filippenko A. V., 2003a, PASP, 115, 1
Van Dyk S. D., Li W., Filippenko A. V., 2003b, PASP, 115, 1289
Van Dyk S. D., Cenko S. B., Silverman J. M., Miller A. A., Filippenko A. V., Bloom J. S., Nugent P. E., 2012, Astron. Telegram, 3971, 1
Vanbeveren D., De Donder E., van Bever J., van Rensbergen W., De Loore C., 1998, New Astron., 3, 443
Vanbeveren D., Van Bever J., Belkus H., 2007, ApJ, 662, L107
Vinkò J., Marion G. H., Wheeler J. C., Foley R. J., Kirshner R. P., Rostopchin S., 2010, CBET, 2300, 1
Walborn N. R., Lasker B. M., Laidler V. G., Chu Y.-H., 1987, ApJ, 321, L41
Wang L., Baade D., Höflich P., Wheeler J. C., 2003, ApJ, 592, 457
Xu D. W., Qiu Y. L., 2001, IAU Circ., 7555, 2
Yoon S.-C., Cantiello M., 2010, ApJ, 717, L62
Yoon S.-C., Langer N., Norman C., 2006, A&A, 460, 199
Yoon S.-C., Woosley S. E., Langer N., 2010, ApJ, 725, 940
Yoon S.-C., Gräfener G., Vink J. S., Kozyreva A., Izzard R. G., 2012, A&A, 544, 11

APPENDIX A: COMPLETE LIST OF SNE EMPLOYED IN THE SURVEY FOR PROGENITORS

Table A1. CCSNe discovered between 1998 and 2012.25 in galaxies with recessional velocities less than 2000 km s^{-1}. The *HST* FOV column notes if the host galaxy has been observed by *HST* prior to explosion and if the position of the SN is 'in' or 'out' of the camera FOV.

Supernova	Galaxy	$V_{\rm vir}$	Type	*HST* FOV	Comments
Core-collapse					
1998A	IC 2627	1974	IIpec	–	Pastorello et al. (2005)SN1987A-like
1998S	NGC 3877	1115	IIn	–	Fassia et al. (2001)
1998bm	IC 2458	1810	II	–	Li et al. (1998), unknown subtype
1998bv	PGC2302994	1794	IIP	–	Kniazeb (1998)
1998dl	NGC 1084	1298	IIP	–	Filippenko & De Breuck (1998a)
...	...	...	...	...	...

Full table available online only.

SUPPORTING INFORMATION

Additional Supporting Information may be found in the online version of this article:

Table A1. CCSNe discovered between 1998 and 2012.25 in galaxies with recessional velocities less than 2000 km s^{-1}. The *HST* FOV column notes if the host galaxy has been observed by *HST* prior to explosion and if the position of the SN is 'in' or 'out' of the camera FOV (http://mnras.oxfordjournals.org/lookup/suppl/doi:10.1093/mnras/stt1612/-/DC1).

Please note: Oxford University Press are not responsible for the content or functionality of any supporting materials supplied by the authors. Any queries (other than missing material) should be directed to the corresponding author for the paper.

This paper has been typeset from a TEX/LATEX file prepared by the author.